*Int. J. Solids Structures* Vol. 30, No. 24, pp. 3357–3379, 1993
Printed in Great Britain

0020-7683/93 $6.00+ .00


# A CONTINUUM THREE-DIMENSIONAL VIBRATION ANALYSIS OF THICK RECTANGULAR PLATES

K. M. LIEW, K. C. HUNG and M. K. LIM
Dynamics and Vibration Centre, School of Mechanical and Production Engineering,
Nanyang Technological University, Nanyang Avenue, Singapore 2263, Republic of Singapore

(*Received* 9 *February* 1993; *in revised form* 28 *June* 1993)

**Abstract**—This paper presents a continuum three-dimensional Ritz formulation for the vibration analysis of homogeneous, thick, rectangular plates with arbitrary combinations of boundary constraints. This model is formulated on the basis of the linear, three-dimensional, small deformation elasticity theory to predict the vibratory responses of these thick rectangular plates. The displacement fields in the transverse and in-plane directions are expressed by sets of orthogonally generated polynomial functions. These shape functions are intrinsically a product of a class of orthogonal polynomial functions and a basic function which are chosen to satisfy the essential geometric boundary conditions at the outset. Sets of frequency data for plates with various aspect ratios and thickness ratios have been presented. These data are used to examine the merits and limitations of the classical plate theory and Mindlin plate theory by direct comparisons. Finally, using the three-dimensional continuum approach, sets of first known deformed mode shapes have been generated thus helping to understand the vibratory motion. Furthermore, these results may also serve as the benchmark to further research into the refined plate theories.

## 1. INTRODUCTION

To date, closed-form analytical solutions to the eigenvalue problems associated with the elastic continuum are limited to only simple cases. To seek practical solutions, many researchers have resorted to numerical approximations. As known, for elastic continuums of various geometries and boundary conditions, the Ritz energy method can provide accurate solutions, however, it depends largely on the choice of global admissible functions.

Well known existing functions have been expressed in terms of finite series such as trigonometric functions (Young, 1950; Warburton, 1954), power series expansion (Narita, 1985) and hill functions (Kao, 1973). They have been used with great success in the past, mainly for thin plates. Lately, sets of self-generating polynomial functions have been proposed and implemented in the Ritz procedure for various thin plate problems (Bhat, 1985; Liew *et al.*, 1990). Liew and his co-workers (1993) have recently extended the polynomial-based Ritz formulation to Mindlin's plates. The advantage of these polynomials, as pointed out (Liew *et al.*, 1990), is mainly due to the ease of generation and numerical implementation that greatly enhance the computational efficiency of the Ritz method. With this merit, it is envisaged that the formidable efforts involved in three-dimensional computations can be drastically reduced.

The complexity of three-dimensional analysis has led to the development of refined plate theories (Levinson, 1980; Reddy, 1984). These theories aim to reduce the dimensions of problems (and thus the determinant size of the eigenvalue equation) from three to two by addressing the quantities of interest, such as membrane forces, bending moments and shear forces, in terms of certain averages over the displacement across the smaller dimension, i.e. thickness dimension. These simplifications are inherently erroneous and result in erroneous responses of structures. The discrepancies become significant when the thickness dimension increases to that comparable to the other leading plate dimensions.

Very often, plates used in industrial situations are moderately thick or very thick. They can be found in many engineering applications such as civil, structural, military and marine structures. Due to the practical importance, solution methods that can provide reliable and accurate results will be of tremendous help to our understanding of their dynamic characteristics. Moreover, in order to assess the accuracy of simple plate theories, accurate three-dimensional solutions to these problems will be of advantage if available for direct comparison. Such closed-form exact solutions have been derived notably by Srinivas *et al.*

(1970) and Wittrick (1987) for simply supported thick rectangular plates. For other boundary conditions, solutions based on three-dimensional elasticity theory are available only for cantilevered parallelepipeds due to the excellent work of Leissa and Zhang (1983).

Three-dimensional analysis of thick plates subject to other support conditions is not found in current literature. This study attempts to fill this apparent void by providing sets of first known frequency data and three-dimensional deformed mode shapes for thick plates subject to different boundary constraints. The natural vibratory motions have been manifested into three-dimensional deformed mesh plots to depict vividly the contribution of each displacement component to the deformed geometry. This study covers five practical sets of boundary conditions, various aspect ratios and side-to-thickness ratios. The reported deflection contour plots and three-dimensional deformed mode shapes serve to enhance our understanding and visualization of the vibratory characteristics of these plates. The present solutions supplement the existing database, and further serve as the benchmark for researchers to examine the merits of new development in refined plate theories.

## 2. THEORETICAL FORMULATION

### 2.1. *Three-dimensional elasticity theory*

Consider a homogeneous, thick, rectangular plate, as shown in Fig. 1, bounded by the edges $-a/2 \leqslant x \leqslant a/2$, $-b/2 \leqslant y \leqslant b/2$ and $-t/2 \leqslant z \leqslant t/2$. Stress free surfaces are assumed at $z = -t/2$ and $t/2$. The origin of the coordinate system is taken to be at the geometric center of the plate. To determine the vibration frequencies and mode shapes of the plate, the Ritz energy procedure is followed. The deflections are decomposed into three orthogonal displacement components, $u$, $v$ and $w$ parallel to the $x$-, $y$- and $z$-directions, respectively.

For small amplitude vibratory motion, the strain energy of elastic plates in terms of the displacement fields, $\{u, v, w\}^T$ can be expressed as:

$$\mathbb{U} = \frac{1}{2}\int_v [\varepsilon]^T \mathbf{D} [\varepsilon] \, dV, \tag{1}$$

where $[\varepsilon]$ is the strain tensor:

$$[\varepsilon] = \begin{Bmatrix} \varepsilon_x \\ \varepsilon_y \\ \varepsilon_z \\ \gamma_{xy} \\ \gamma_{xz} \\ \gamma_{yz} \end{Bmatrix} = \begin{bmatrix} \partial/\partial x & 0 & 0 \\ 0 & \partial/\partial y & 0 \\ 0 & 0 & \partial/\partial z \\ \partial/\partial y & \partial/\partial x & 0 \\ \partial/\partial z & 0 & \partial/\partial x \\ 0 & \partial/\partial z & \partial/\partial y \end{bmatrix} \begin{Bmatrix} u \\ v \\ w \end{Bmatrix}. \tag{2}$$

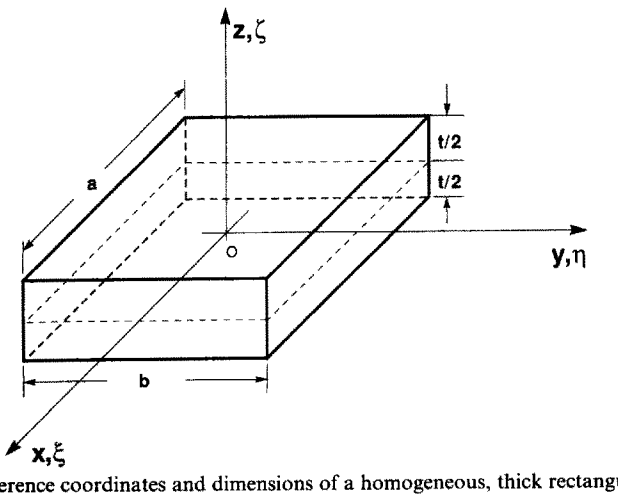


Fig. 1. Reference coordinates and dimensions of a homogeneous, thick rectangular plate.

For an isotropic material, the elasticity matrix **D** is given by:

$$\mathbf{D} = \frac{E(1-v)}{(1+v)(1-2v)} \begin{bmatrix} 1 & v/(1-v) & v/(1-v) & 0 & 0 & 0 \\ & 1 & v/(1-v) & 0 & 0 & 0 \\ & & 1 & 0 & 0 & 0 \\ & & & \frac{(1-2v)}{2(1-v)} & 0 & 0 \\ & & & & \frac{(1-2v)}{2(1-v)} & 0 \\ \text{symmetric} & & & & & \frac{(1-2v)}{2(1-v)} \end{bmatrix}, \quad (3)$$

where $E$ is the modulus of elasticity and $v$ is Poisson's ratio.

The kinetic energy for free vibration is given by,

$$\mathbb{T} = \frac{\rho}{2} \int_v (\dot{u}^2 + \dot{v}^2 + \dot{w}^2)\, dv, \quad (4)$$

where $\dot{u}$, $\dot{v}$ and $\dot{w}$ are the corresponding velocity components in the $x$-, $y$- and $z$-directions, respectively, and $\rho$ is the mass density per unit volume.

The boundary conditions for the stress free surfaces at $z = -t/2$ and $t/2$ can be expressed in terms of the spatial displacement components as follows,

$$\sigma_z = \Lambda e + 2G\left(\frac{\partial u}{\partial z}\right) = 0; \quad \text{at} \quad z(-t/2;\, t/2), \quad (5a)$$

$$\tau_{xz} = G\left(\frac{\partial w}{\partial x} + \frac{\partial u}{\partial z}\right) = 0; \quad \text{at} \quad z(-t/2;\, t/2), \quad (5b)$$

$$\tau_{yz} = G\left(\frac{\partial w}{\partial y} + \frac{\partial v}{\partial z}\right) = 0; \quad \text{at} \quad z(-t/2;\, t/2), \quad (5c)$$

where $e$ is the dilatation given by:

$$e = \left(\frac{\partial}{\partial x}; \frac{\partial}{\partial y}; \frac{\partial}{\partial z}\right)\{u, v, w\}^T, \quad (6)$$

and $\Lambda$ and $G$ are the Lamé constants given by:

$$\Lambda = \frac{vE}{(1+v)(1-2v)}; \quad G = \frac{E}{2(1+v)}. \quad (7)$$

The displacement vectors $\{u, v, w\}^T$ are each expressed in terms of functions in $x$, $y$, $z$ and $\bar{\tau}$:

$$u = u(x, y, z, \bar{\tau}) = U(x, y, z)e^{i\omega\bar{\tau}}, \quad (8a)$$

$$v = v(x, y, z, \bar{\tau}) = V(x, y, z)e^{i\omega\bar{\tau}}, \quad (8b)$$

$$w = w(x, y, z, \bar{\tau}) = W(x, y, z)e^{i\omega\bar{\tau}}, \quad (8c)$$

in which $\bar{\tau}$ is time and $\omega$ denotes the frequency of vibration.

2.2. *The Ritz energy method*

For simplicity and generality, a nondimensional coordinate system is introduced:

$$\xi = \frac{x}{a}; \quad \eta = \frac{y}{b} \quad \text{and} \quad \zeta = \frac{z}{t}, \tag{9}$$

where $a$ and $b$ are the length and width of the rectangular planform (see Fig. 1), and $t$ is the thickness dimension of the plate. The in-plane and transverse deflection amplitude functions, $U(\xi,\eta,\zeta)$, $V(\xi,\eta,\zeta)$ and $W(\xi,\eta,\zeta)$ in eqns (8) can be approximated by a set of separable orthogonal polynomial functions in $\xi$, $\eta$ and $\zeta$, respectively,

$$U(\xi,\eta,\zeta) = \sum^{I}\sum^{J}\sum^{K} C_{uijk}\phi_{ui}(\xi)\psi_{uj}(\eta)\chi_{uk}(\zeta), \tag{10a}$$

$$V(\xi,\eta,\zeta) = \sum^{L}\sum^{M}\sum^{N} C_{vlmn}\phi_{vl}(\xi)\psi_{vm}(\eta)\chi_{vn}(\zeta), \tag{10b}$$

$$W(\xi,\eta,\zeta) = \sum^{P}\sum^{Q}\sum^{R} C_{wpqr}\phi_{wp}(\xi)\psi_{wq}(\eta)\chi_{wr}(\zeta), \tag{10c}$$

where $C_{uijk}$, $C_{vlmn}$ and $C_{wpqr}$ are the undetermined coefficients and $\phi$, $\psi$ and $\chi$ are the corresponding polynomial functions. The functions are basically sets of orthogonally generated polynomials to be discussed in due course.

Let the maximum energy functional of the thick rectangular plate be,

$$\mathbb{F} = \mathbb{U}_{\max} - \mathbb{T}_{\max}, \tag{11}$$

in which $\mathbb{U}_{\max}$, the maximum strain energy, and $\mathbb{T}_{\max}$, the maximum kinetic energy, occur respectively at maximum deflection and maximum velocity in a vibratory cycle.

Substituting the spatial displacement functions given in eqn (10) into the energy functional and minimizing with respect to the unknown coefficients according to the Ritz procedure:

$$\partial\mathbb{F}/\partial C_{uijk} = 0, \tag{12a}$$

$$\partial\mathbb{F}/\partial C_{vlmn} = 0, \tag{12b}$$

$$\partial\mathbb{F}/\partial C_{wpqr} = 0, \tag{12c}$$

leads to the governing eigenvalue equation:

$$\left(\begin{bmatrix} [\mathbf{K}_{uu}] & [\mathbf{K}_{uv}] & [\mathbf{K}_{uw}] \\ & [\mathbf{K}_{vv}] & [\mathbf{K}_{vw}] \\ \text{symmetric} & & [\mathbf{K}_{ww}] \end{bmatrix} - \bar{\lambda}^2 \begin{bmatrix} [\mathbf{M}_{uu}] & 0 & 0 \\ & [\mathbf{M}_{vv}] & 0 \\ \text{symmetric} & & [\mathbf{M}_{ww}] \end{bmatrix}\right) \begin{Bmatrix} \{\mathbf{C}_u\} \\ \{\mathbf{C}_v\} \\ \{\mathbf{C}_w\} \end{Bmatrix} = \begin{Bmatrix} \{0\} \\ \{0\} \\ \{0\} \end{Bmatrix}, \tag{13}$$

in which $[\mathbf{K}_{ij}]$ is the stiffness matrix; $[\mathbf{M}_{ij}]$ is the diagonal mass matrix; and $\{\mathbf{C}_u\}$, $\{\mathbf{C}_v\}$ and $\{\mathbf{C}_w\}$ are the column vectors of the unknown coefficients which can be expressed in the following forms:

$$\{\mathbf{C}_u\} = \begin{Bmatrix} C_{u111} \\ C_{u112} \\ \vdots \\ C_{u11K} \\ C_{u121} \\ \vdots \\ C_{u1JK} \\ C_{u211} \\ \vdots \\ C_{uIJK} \end{Bmatrix}; \quad \{\mathbf{C}_v\} = \begin{Bmatrix} C_{v111} \\ C_{v112} \\ \vdots \\ C_{v11N} \\ C_{v121} \\ \vdots \\ C_{v1MN} \\ C_{v211} \\ \vdots \\ C_{vLMN} \end{Bmatrix} \text{and} \quad \{\mathbf{C}_w\} = \begin{Bmatrix} C_{w111} \\ C_{w112} \\ \vdots \\ C_{w11R} \\ C_{w121} \\ \vdots \\ C_{w1QR} \\ C_{w211} \\ \vdots \\ C_{wPQR} \end{Bmatrix}. \tag{14}$$

The expressions of the various elements in the stiffness matrix [K] and mass matrix [M] are given by:

$$[\mathbf{K}_{uu}] = \frac{1-\nu}{(1-2\nu)} E^{11}_{uiu\bar{i}} F^{00}_{uju\bar{j}} G^{00}_{uku\bar{k}} + \frac{1}{2}\left(\frac{a}{b}\right)^2 E^{00}_{uiu\bar{i}} F^{11}_{uju\bar{j}} G^{00}_{uku\bar{k}} + \frac{1}{2}\left(\frac{a}{c}\right)^2 E^{00}_{uiu\bar{i}} F^{00}_{uju\bar{j}} G^{11}_{uku\bar{k}}, \tag{15a}$$

$$[\mathbf{K}_{uv}] = \left(\frac{a}{b}\right)\left(\frac{\nu}{(1-2\nu)} E^{10}_{uivl} F^{01}_{ujvm} G^{00}_{ukvn} + \tfrac{1}{2} E^{00}_{uivl} F^{10}_{ujvm} G^{00}_{ukvn}\right), \tag{15b}$$

$$[\mathbf{K}_{uw}] = \left(\frac{a}{c}\right)\frac{\nu}{(1-2\nu)} E^{10}_{uiwp} F^{00}_{ujwq} G^{01}_{ukwr} + \frac{1}{2}\left(\frac{a}{b}\right) E^{01}_{uiwp} F^{00}_{ujwq} G^{10}_{ukwr}, \tag{15c}$$

$$[\mathbf{K}_{vv}] = \left(\frac{a}{b}\right)^2 \frac{1-\nu}{(1-2\nu)} E^{00}_{vlv\bar{l}} F^{11}_{vmv\bar{m}} G^{00}_{vnv\bar{n}} + \frac{1}{2}\left(\frac{a}{c}\right)^2 E^{00}_{vlv\bar{l}} F^{00}_{vmv\bar{m}} G^{11}_{vnv\bar{n}} + \tfrac{1}{2} E^{11}_{vlv\bar{l}} F^{00}_{vmv\bar{m}} G^{00}_{vnv\bar{n}}, \tag{15d}$$

$$[\mathbf{K}_{vw}] = \left(\frac{a^2}{bc}\right)\left(\frac{\nu}{(1-2\nu)} E^{00}_{vlwp} F^{10}_{vmwq} G^{01}_{vnwr} + E^{00}_{vlwp} F^{01}_{vmwq} G^{10}_{vnwr}\right), \tag{15e}$$

$$[\mathbf{K}_{ww}] = \left(\frac{a}{c}\right)^2 \frac{1-\nu}{(1-2\nu)} E^{00}_{wpw\bar{p}} F^{00}_{wqw\bar{q}} G^{11}_{wrw\bar{r}} + \frac{1}{2}\left(\frac{a}{c}\right)^2 E^{00}_{wpw\bar{p}} F^{11}_{wqw\bar{q}} G^{00}_{wrw\bar{r}} + \tfrac{1}{2} E^{11}_{wpw\bar{p}} F^{00}_{wqw\bar{q}} G^{00}_{wrw\bar{r}}, \tag{15f}$$

$$[\mathbf{M}_{uu}] = (1+\nu) E^{00}_{uiu\bar{i}} F^{00}_{uju\bar{j}} G^{00}_{uku\bar{k}}, \tag{15g}$$

$$[\mathbf{M}_{vv}] = (1+\nu) E^{00}_{vlv\bar{l}} F^{00}_{vmv\bar{m}} G^{00}_{vnv\bar{n}}, \tag{15h}$$

$$[\mathbf{M}_{ww}] = (1+\nu) E^{00}_{wpw\bar{p}} F^{00}_{wqw\bar{q}} G^{00}_{wrw\bar{r}}. \tag{15i}$$

The product of integrals in eqns (15) is given by:

$$E^{rs}_{\alpha l \beta i} = \int_{-0.5}^{0.5} \left[\frac{\mathrm{d}^r \phi_{\alpha l}(\xi)}{\mathrm{d}\xi^r} \frac{\mathrm{d}^s \phi_{\beta i}(\xi)}{\partial \xi^s}\right] \mathrm{d}\xi, \tag{16a}$$

$$F^{rs}_{\alpha m \beta j} = \int_{-0.5}^{0.5} \left[\frac{\mathrm{d}^r \psi_{\alpha m}(\eta)}{\mathrm{d}\eta^r} \frac{\mathrm{d}^s \psi_{\beta j}(\eta)}{\partial \eta^s}\right] \mathrm{d}\eta, \tag{16b}$$

$$G^{rs}_{\alpha n \beta k} = \int_{-0.5}^{0.5} \left[\frac{\mathrm{d}^r \chi_{\alpha n}(\zeta)}{\mathrm{d}\zeta^r} \frac{\mathrm{d}^s \chi_{\beta k}(\zeta)}{\partial \zeta^s}\right] \mathrm{d}\zeta, \tag{16c}$$

where $r, s = 0, 1$ and subscripts $\alpha, \beta$ represent the corresponding displacement fields in $u, v$ and $w$. Solving the characteristic eigenvalue problem defined by eqn (13) yields the frequency parameter, $\bar{\lambda} = \omega a(\rho/E)^{1/2}$. This parameter can be expressed in the form of $\lambda = (\omega b^2/\pi^2)(\rho t/D)^{1/2}$ by multiplying $\bar{\lambda}$ with the following factor,

$$\lambda = \frac{b^2}{at\pi^2} \{12(1-\nu^2)\}^{1/2} \bar{\lambda}. \tag{17}$$

### 2.3. *Orthogonal functions and boundary conditions*

The set of polynomial functions representing the spatial displacements of the continuum is orthogonalized via the Gram–Schmidt process (Chihara, 1978). This is illustrated for $\phi(\xi)$ as follows,

$$\phi_{k+1}(\xi) = \{g(\xi) - \theta_k\}\phi_k(\xi) - \Xi_k \phi_{k-1}(\xi); \quad k = 1, 2, 3, \ldots, \tag{18}$$

where

$$\Theta_k = \frac{\int_{-0.5}^{0.5} g(\xi)\phi_k^2(\xi)\,\mathrm{d}\xi}{\int_{-0.5}^{0.5} \phi_k^2(\xi)\,\mathrm{d}\xi}, \tag{19a}$$

and

$$\Xi_k = \frac{\int_{-0.5}^{0.5} \phi_k^2(\xi)\,\mathrm{d}\xi}{\int_{-0.5}^{0.5} \phi_{k-1}^2(\xi)\,\mathrm{d}\xi}. \tag{19b}$$

The polynomial $\phi_0(\xi)$ is defined as zero. Note that the coefficients, $\Theta_k$ and $\Xi_k$ for the subsequent term can be computed from the two previous polynomials.

The set of polynomials generated satisfies the following orthogonality condition:

$$\int_{-0.5}^{0.5} \phi_i(\xi)\phi_j(\xi)\,\mathrm{d}\xi = n_{ij}\delta_{ij}, \tag{20}$$

where $\delta_{ij}$ is the Kronecker delta and the value of $n_{ij}$ depends on the normalization used. The generating function, $g(\xi)$, is chosen such that the higher terms continue to satisfy the geometric boundary conditions. Polynomials in the $y$- and $z$-directions can also be constructed by following a similar procedure.

In this analysis, the boundary conditions are chosen such that $xz$- and $yz$-planes are the symmetry planes. This symmetry consideration permits the classification of the vibration modes into four distinct symmetry classes. Namely, doubly symmetric (SS) modes, symmetric–antisymmetric modes (SA), antisymmetric–symmetric modes (AS) and double antisymmetric modes (AA) about these $xz$- and $yz$-planes. The apparent computational advantage of this classification is that it reduces the determinant size of the resulting eigenvalue equation to that manageable by smaller computers.

The basic function in the $z$-direction, $\chi(\zeta)$, is chosen to be unity [$\chi(\zeta) = 1$]. It satisfies the essential geometric requirement of the stress free surfaces at $z = -t/2$ and $t/2$. In $x$- or $y$-direction, it depends on the boundary constraints and symmetry classes of vibration, the basic functions in these directions take on different forms. For a stress free surface on a straight edge, $x$ = constant, the boundary requirements are;

$$\sigma_x = 0, \quad \tau_{xy} = 0 \quad \text{and} \quad \tau_{xz} = 0. \tag{21}$$

On the other hand, for a simple support on the same straight edge, the corresponding boundary conditions are:

$$w = 0, \quad v = 0 \quad \text{and} \quad \sigma_x = 0. \tag{22}$$

Finally, for a fully clamped edge, the boundary conditions are:

$$w = 0, \quad v = 0 \quad \text{and} \quad u = 0. \tag{23}$$

In the Ritz formulation, it is sufficient to choose admissible functions that satisfy only the essential geometric boundary conditions. Tables 1(a) and 1(b) summarize the respective basic functions used in each of the symmetry classes at different boundary conditions.

Table 1(a). Notations for various boundary conditions and the corresponding basic functions in the $x$-direction

| Boundary conditions | $f_0(\xi)$ | $f_e(\xi)$ |
|---|---|---|
| Free–free ($F$–$F$) | $\phi_{u1}(\xi)=\xi$<br>$\sigma_{v1}(\xi)=\xi$<br>$\phi_{w1}(\xi)=\xi$ | $\phi_{u1}(\xi)=1.0$<br>$\phi_{v1}(\xi)=1.0$<br>$\phi_{w1}(\xi)=1.0$ |
| Simply–simply supports ($S$–$S$) | $\phi_{u1}(\xi)=\xi$<br>$\phi_{v1}(\xi)=\xi^3-0.25\xi$<br>$\phi_{w1}(\xi)=\xi^3-0.25\xi$ | $\phi_{u1}(\xi)=1.0$<br>$\phi_{v1}(\xi)=\xi^2-0.25$<br>$\phi_{w1}(\xi)=\xi^2-0.25$ |
| Clamped–clamped ($C$–$C$) | $\phi_{u1}(\xi)=\xi^3-0.25\xi$<br>$\phi_{v1}(\xi)=\xi^3-0.25\xi$<br>$\phi_{w1}(\xi)=\xi^3-0.25\xi$ | $\phi_{u1}(\xi)=\xi^2-0.25$<br>$\phi_{v1}(\xi)=\xi^2-0.25$<br>$\phi_{w1}(\xi)=\xi^2-0.25$ |

Table 1(b). Basic functions for $U$, $V$ and $W$ components at different symmetry classes

| Symmetry class | $U$ | | $V$ | | $W$ | |
|---|---|---|---|---|---|---|
| | $\phi_{u1}(\xi)$ | $\psi_{u1}(\eta)$ | $\phi_{v1}(\xi)$ | $\psi_{v1}(\eta)$ | $\phi_{w1}(\xi)$ | $\psi_{w1}(\eta)$ |
| $SS$ | $f_o$ | $f_e$ | $f_e$ | $f_o$ | $f_e$ | $f_e$ |
| $AS$ | $f_e$ | $f_e$ | $f_o$ | $f_o$ | $f_o$ | $f_e$ |
| $SA$ | $f_o$ | $f_o$ | $f_e$ | $f_e$ | $f_e$ | $f_o$ |
| $AA$ | $f_e$ | $f_o$ | $f_o$ | $f_e$ | $f_o$ | $f_o$ |
| | Generating function $g(\xi;\eta;\zeta)=(\xi^2;\eta^2;\zeta)$ | | | | | |

## 3. VERIFICATION AND NUMERICAL APPLICATIONS

The three-dimensional continuum method described in the previous section has been applied to compute the nondimensional frequency parameters, $\lambda=(\omega b^2/\pi^2)(\rho t/D)^{1/2}$ and vibration mode shapes for the homogeneous, thick, rectangular plates subject to arbitrary combinations of boundary constraints. The notation for boundary conditions, for instance, SFCF denotes a rectangular plate with edges $x=-a/2$, $y=-b/2$, $x=a/2$ and $y=b/2$ having the simply supported, free, clamped, and free support conditions, respectively. This boundary convention is used throughout the present study.

### 3.1. *Convergence and comparison of eigenvalues*

Table 2(a) presents the convergence studies on the eigenvalues $\lambda$ for simply supported square plates. The rate of convergence is examined for the plates with thickness ratios, $t/b=0.01$, 0.1 and 0.5. The numbers of terms used in the triple infinite series of $U$, $V$ and $W$ are stepped steadily from $4\times4\times3$ to higher terms to demonstrate the monotonic downward convergence behavior of $\lambda$.

A careful scrutiny of the convergence table reveals that as the thickness ratio increases, the number of terms needed for the polynomial function in the thickness direction ($z$-direction) increases proportionally. For a relatively thin plate ($t/b=0.01$), 4 terms in the $z$-direction are sufficient to give converged results up to five significant figures. However, it needs as high as seven terms for a plate with thickness ratio $t/b=0.5$ to achieve the same degree of accuracy. On the other hand, the number of terms needed in the shape functions along the plate surface ($x$- and $y$-directions) reduces drastically from $7\times7$ to $4\times4$ terms as the plate thickness dimension becomes significant. Consequently, the overall determinant size involved in the solution of thicker rectangular plates becomes smaller (det = 336 for a plate with $t/b=0.5$ as compared to det = 558 for a plate with $t/b=0.01$). To investigate the convergence behaviors with respect to the boundary conditions, frequency parameters for a moderately thick square plate are computed ($t/b=0.1$). The rate of convergence for each boundary condition is presented in Table 2(b). The convergence patterns are found to be invariant with respect to the boundary constraints.

From the preceding convergence studies, it was established that for very thin plates ($t/b=0.01$), $9\times9\times4$ terms were needed to achieve a reasonable convergence. For plates

Table 2(a). Convergence of frequency parameters, $\lambda = (\omega b^2/\pi^2)(\rho t/D)^{1/2}$, for a thick square plate with SSSS boundary condition

| Thickness ratio, $t/b$ | Terms in $x, y, z$ | Det size | Symmetry classes and mode number | | | | | | | | |
|---|---|---|---|---|---|---|---|---|---|---|---|
| | | | SS-1 | SS-2 | SS-3 | SA-1† | SA-2† | SA-3† | AA-1 | AA-2 | AA-3 |
| 0.01 | 4×4×3 | 144 | 1.9994 | 9.9864 | 9.9864 | 4.9961 | 12.975 | 17.631 | 7.9900 | 20.563 | 20.563 |
| | 4×4×4 | 192 | 1.9993 | 9.9847 | 9.9847 | 4.9957 | 12.972 | 17.625 | 7.9889 | 20.555 | 20.555 |
| | 4×4×5 | 240 | 1.9993 | 9.9847 | 9.9847 | 4.9957 | 12.972 | 17.625 | 7.9889 | 20.555 | 20.555 |
| | 5×5×4 | 300 | 1.9993 | 9.9826 | 9.9826 | 4.9956 | 12.971 | 16.971 | 7.9888 | 19.950 | 19.950 |
| | 6×6×4 | 432 | 1.9993 | 9.9826 | 9.9826 | 4.9956 | 12.971 | 16.950 | 7.9888 | 19.931 | 19.931 |
| | 7×7×4 | 588 | 1.9993 | 9.9826 | 9.9826 | 4.9956 | 12.971 | 16.950 | 7.9888 | 19.930 | 19.930 |
| | 8×8×4 | 768 | 1.9993 | 9.9826 | 9.9826 | 4.9956 | 12.971 | 16.950 | 7.9888 | 19.930 | 19.930 |
| | 9×9×4 | 972 | 1.9993 | 9.9826 | 9.9826 | 4.9956 | 12.971 | 16.950 | 7.9888 | 19.930 | 19.930 |
| 0.1 | 4×4×3 | 144 | 1.9403 | 8.7672 | 8.7672 | 4.6546 | 6.5234 | 11.037 | 7.1754 | 13.047 | 13.047 |
| | 5×5×4 | 300 | 1.9342 | 8.6631 | 8.6631 | 4.6224 | 6.5234 | 10.882 | 7.1038 | 13.047 | 13.047 |
| | 6×6×4 | 432 | 1.9342 | 8.6631 | 8.6631 | 4.6224 | 6.5234 | 10.882 | 7.1038 | 13.047 | 13.047 |
| | 5×5×5 | 375 | 1.9342 | 8.6617 | 8.6617 | 4.6222 | 6.5234 | 10.879 | 7.1030 | 13.047 | 13.047 |
| | 5×5×6 | 450 | 1.9342 | 8.6617 | 8.6617 | 4.6222 | 6.5234 | 10.879 | 7.1030 | 13.047 | 13.047 |
| | 5×5×7 | 525 | 1.9342 | 8.6617 | 8.6617 | 4.6222 | 6.5234 | 10.879 | 7.1030 | 13.047 | 13.047 |
| | 5×5×8 | 600 | 1.9342 | 8.6617 | 8.6617 | 4.6222 | 6.5234 | 10.879 | 7.1030 | 13.047 | 13.047 |
| | 5×5×9 | 675 | 1.9342 | 8.6617 | 8.6617 | 4.6222 | 6.5234 | 10.879 | 7.1030 | 13.047 | 13.047 |
| 0.5 | 4×4×3 | 144 | 1.2964 | 1.8451 | 2.9678 | 1.3047 | 2.4255 | 2.9174 | 2.6094 | 2.6094 | 3.2489 |
| | 4×4×4 | 192 | 1.2613 | 1.8451 | 2.9337 | 1.3047 | 2.3440 | 2.9174 | 2.6094 | 2.6094 | 3.1361 |
| | 5×5×4 | 300 | 1.2613 | 1.8451 | 2.9337 | 1.3047 | 2.3440 | 2.9174 | 2.6094 | 2.6094 | 3.1361 |
| | 4×4×5 | 240 | 1.2590 | 1.8451 | 2.9326 | 1.3047 | 2.3316 | 2.9174 | 2.6094 | 2.6094 | 3.1093 |
| | 4×4×6 | 288 | 1.2590 | 1.8451 | 2.9325 | 1.3047 | 2.3312 | 2.9174 | 2.6094 | 2.6094 | 3.1081 |
| | 4×4×7 | 336 | 1.2590 | 1.8451 | 2.9325 | 1.3047 | 2.3312 | 2.9174 | 2.6094 | 2.6094 | 3.1080 |
| | 4×4×8 | 384 | 1.2590 | 1.8451 | 2.9325 | 1.3047 | 2.3312 | 2.9174 | 2.6094 | 2.6094 | 3.1080 |
| | 4×4×9 | 432 | 1.2590 | 1.8451 | 2.9325 | 1.3047 | 2.3312 | 2.9174 | 2.6094 | 2.6094 | 3.1080 |

† For a thick square plate with SSSS boundary condition, the frequency parameters, $\lambda$, for SA and AS modes are identical.

Table 2(b). Convergence of frequency parameters, $\lambda = (\omega b^2/\pi^2)(\rho t/D)^{1/2}$, for a thick square plate with different boundary conditions ($t/b = 0.1$)

| Boundary conditions | Terms in $x, y, z$ | Det size | Symmetry classes and mode number | | | | | | | | | | | |
|---|---|---|---|---|---|---|---|---|---|---|---|---|---|---|
| | | | SS-1 | SS-2 | SS-3 | SA-1 | SA-2 | SA-3 | AS-1 | AS-2 | AS-3 | AA-1 | AA-2 | AA-3 |
| SFSF | 4×4×3 | 144 | 0.9591 | 3.4635 | 7.8939 | 3.7158 | 6.3960 | 13.047 | 1.5678 | 4.9400 | 6.7932 | 4.3814 | 6.5234 | 9.5634 |
| | 5×5×4 | 300 | 0.9571 | 3.4370 | 7.8007 | 3.6922 | 6.3185 | 12.869 | 1.5605 | 4.9400 | 6.7297 | 4.3459 | 6.5234 | 9.4286 |
| | 6×6×4 | 432 | 0.9571 | 3.4362 | 7.8001 | 3.6920 | 6.3168 | 12.854 | 1.5604 | 4.9400 | 6.7293 | 4.3456 | 6.5234 | 9.4275 |
| | 5×5×5 | 375 | 0.9571 | 3.4361 | 7.8000 | 3.6920 | 6.3165 | 12.854 | 1.5603 | 4.9400 | 6.7293 | 4.3455 | 6.5234 | 9.4274 |
| | 5×5×6 | 450 | 0.9571 | 3.4361 | 7.7991 | 3.6919 | 6.3162 | 12.850 | 1.5603 | 4.9400 | 6.7287 | 4.3454 | 6.5234 | 9.4259 |
| | 5×5×7 | 525 | 0.9571 | 3.4361 | 7.7990 | 3.6919 | 6.3161 | 12.849 | 1.5603 | 4.9400 | 6.7287 | 4.3454 | 6.5234 | 9.4257 |
| | 5×5×8 | 600 | 0.9571 | 3.4361 | 7.7990 | 3.6919 | 6.3161 | 12.849 | 1.5603 | 4.9400 | 6.7287 | 4.4354 | 6.5234 | 9.4257 |
| | 5×5×9 | 675 | 0.9571 | 3.4361 | 7.7990 | 3.6919 | 6.3161 | 12.849 | 1.5603 | 4.9400 | 6.7287 | 4.3454 | 6.5234 | 9.4257 |
| CFCF | 4×4×3 | 144 | 2.1305 | 3.9777 | 9.9613 | 5.4816 | 7.5064 | 10.648 | 2.4821 | 5.9547 | 7.0530 | 5.9349 | 10.266 | 10.965 |
| | 5×5×4 | 300 | 2.1076 | 3.9268 | 9.7418 | 5.3930 | 7.3674 | 10.640 | 2.4516 | 5.9515 | 6.9708 | 5.8346 | 10.080 | 10.962 |
| | 6×6×4 | 432 | 2.1058 | 3.9246 | 9.7362 | 5.3894 | 7.3625 | 10.637 | 2.4498 | 5.9502 | 6.9695 | 5.8309 | 10.076 | 10.962 |
| | 5×5×5 | 375 | 2.1051 | 3.9240 | 9.7343 | 5.3880 | 7.3611 | 10.635 | 2.4491 | 5.9496 | 6.9692 | 5.8294 | 10.075 | 10.962 |
| | 5×5×6 | 450 | 2.1054 | 3.9240 | 9.7309 | 5.3868 | 7.3593 | 10.636 | 2.4493 | 5.9500 | 6.9684 | 5.8282 | 10.072 | 10.962 |
| | 5×5×7 | 525 | 2.1051 | 3.9234 | 9.7278 | 5.3860 | 7.3582 | 10.636 | 2.4489 | 5.9500 | 6.9678 | 5.8273 | 10.071 | 10.962 |
| | 5×5×8 | 600 | 2.1050 | 3.9234 | 9.7278 | 5.3859 | 7.3582 | 10.636 | 2.4489 | 5.9500 | 6.9678 | 5.8273 | 10.071 | 10.961 |
| | 5×5×9 | 675 | 2.1050 | 3.9234 | 9.7276 | 5.3859 | 7.3581 | 10.636 | 2.4489 | 5.9500 | 6.9678 | 5.8272 | 10.070 | 10.961 |
| SCSC | 4×4×3 | 144 | 2.7490 | 8.9733 | 10.624 | 5.0539 | 6.5234 | 12.455 | 6.1549 | 11.521 | 11.658 | 8.1862 | 13.047 | 15.492 |
| | 5×5×4 | 300 | 2.7212 | 8.8556 | 10.399 | 5.0031 | 6.5234 | 12.195 | 6.0590 | 11.459 | 11.518 | 8.0582 | 13.047 | 15.490 |
| | 6×6×4 | 432 | 2.7198 | 8.8551 | 10.395 | 5.0022 | 6.5234 | 12.191 | 6.0561 | 11.458 | 11.517 | 8.0558 | 13.047 | 15.490 |
| | 5×5×5 | 375 | 2.7192 | 8.8549 | 10.393 | 5.0019 | 6.5234 | 12.190 | 6.0549 | 11.457 | 11.517 | 8.0549 | 13.047 | 15.490 |
| | 5×5×6 | 450 | 2.7193 | 8.8532 | 10.389 | 5.0015 | 6.5234 | 12.184 | 6.0532 | 11.452 | 11.517 | 8.0524 | 13.047 | 15.490 |
| | 5×5×7 | 525 | 2.7189 | 8.8528 | 10.386 | 5.0011 | 6.5234 | 12.181 | 6.0523 | 11.451 | 11.517 | 8.0514 | 13.047 | 15.490 |
| | 5×5×8 | 600 | 2.7189 | 8.8528 | 10.386 | 5.0011 | 6.5234 | 12.181 | 6.0523 | 11.451 | 11.517 | 8.0513 | 13.047 | 15.490 |
| | 5×5×9 | 675 | 2.7188 | 8.8528 | 10.386 | 5.0011 | 6.5234 | 12.181 | 6.0522 | 11.451 | 11.517 | 8.0513 | 13.047 | 15.490 |
| CCCC | 4×4×3 | 144 | 3.3675 | 10.746 | 10.847 | 6.4608 | 12.531 | 13.018 | 6.4608 | 12.531 | 13.018 | 9.0870 | 14.871 | 17.762 |
| | 5×5×4 | 300 | 3.3254 | 10.513 | 10.613 | 6.3536 | 12.525 | 12.724 | 6.3536 | 12.525 | 12.724 | 8.9147 | 14.871 | 17.305 |
| | 6×6×4 | 432 | 3.3231 | 10.508 | 10.608 | 6.3501 | 12.523 | 12.719 | 6.3501 | 12.523 | 12.719 | 8.9104 | 14.870 | 17.299 |
| | 5×5×5 | 375 | 3.3222 | 10.507 | 10.606 | 6.3487 | 12.522 | 12.718 | 6.3487 | 12.522 | 12.718 | 8.9089 | 14.870 | 17.297 |
| | 5×5×6 | 450 | 3.3223 | 10.502 | 10.603 | 6.3470 | 12.522 | 12.710 | 6.3470 | 12.522 | 12.710 | 8.9049 | 14.870 | 17.280 |
| | 5×5×7 | 525 | 3.3216 | 10.499 | 10.598 | 6.3458 | 12.522 | 12.706 | 6.3458 | 12.522 | 12.706 | 8.9031 | 14.870 | 17.275 |
| | 5×5×8 | 600 | 3.3216 | 10.499 | 10.598 | 6.3457 | 12.522 | 12.706 | 6.3457 | 12.522 | 12.706 | 8.9031 | 14.870 | 17.275 |
| | 5×5×9 | 675 | 3.3215 | 10.499 | 10.598 | 6.3457 | 12.522 | 12.706 | 6.3457 | 12.522 | 12.706 | 8.9030 | 14.870 | 17.275 |

with other thickness ratios, it has been found that similar convergence could be attained with polynomials of $6 \times 6 \times 8$ terms. These established polynomial sets are used throughout the present computations.

To validate the accuracy of the present method, comparison studies have been carried out for cases where the solutions for exact three-dimensional analysis and simple plate theories, notably the classical plate theory (CPT) and the shear deformable plate theory (SDPT) are available. For this purpose, thick rectangular plates with simply supported (SSSS) and cantilevered (CFFF) boundaries have been considered. Table 3(a) lists the computed frequency parameters for the simply supported plate together with the known solutions of approximate theories and existing exact three-dimensional analysis. The frequency data for the classical plate theory are obtained from the work of Leissa (1973) and the Mindlin theory's results are quoted from the work of Dawe *et al.* (1985) that used a shear correction factor $\kappa = \pi^2/12$. The three-dimensional results are extracted from the excellent work of Srinivas *et al.* (1970) who pioneered in the exact three-dimensional analysis of simply supported thick plates. From Table 3(a), it is observed that at thickness ratio $t/b = 0.01$, the frequency parameters obtained from the approximate theories and the present three-dimensional analysis are in close agreement. At a higher thickness ratio, $t/b = 0.1$, the classical plate theory, however, tends to give much higher eigenvalues than those of the Mindlin theory and the present three-dimensional analysis. This is attributed to the assumption made in the classical plate theory that a line normal to the plate middle surface remains normal during the deformation. This assumption neglects the effects of through thickness shear deformation and rotary inertia which results in over-estimating the plate stiffness. On the other hand, in the Mindlin plate theory, the shear deformation effects are ingeniously accounted for in the formulation. A shear correction factor, however, is introduced to achieve a more accurate shear strain distribution through the plate thickness. While in the present three-dimensional analysis and the exact three-dimensional analysis of Srinivas *et al.* (1970), this effect has been implicitly incorporated in the elasticity formulation. This has resulted in excellent agreement between the results by the present method with those of Srinivas *et al.* (1970).

For the cantilevered thick rectangular plate, the frequency parameters are compared with those presented by Leissa and Zhang (1983). In this study, the symmetry classification adopted by Leissa and Zhang (1983) has been followed. The first five frequency parameters given in Table 3(b) for each symmetry class are compared with those values of Leissa and Zhang (1983). It can be seen that excellent agreement has also been obtained between both methods.

### 3.2. *Results and discussion*

Having established the rate of convergence and degrees of accuracy of the present formulation, the three-dimensional continuum method is applied to compute the nondimensional frequency parameters, $\lambda = (\omega b^2/\pi^2)(\rho t/D)^{1/2}$, for rectangular plates with various geometric configurations and boundary conditions: SSSS, SFSF, CFCF, SCSC and CCCC. Numerical results are presented in Tables 4(a)–(e) for plates with aspect ratios ranging from 0.5–2.0; and side-to-thickness ratios covering the range of 0.01–0.5. The influences of plate aspect ratio and thickness ratio on the vibration frequencies are examined. The first three nondimensional frequency parameters, $\lambda$, corresponding to each distinct symmetry class were calculated. For all these cases where Poisson's ratio is needed, it is taken to be $\nu = 0.3$.

From these tabulated results, it is observed that for plates with prescribed boundary condition and aspect ratio, the nondimensional frequency parameter, $\lambda$, decreases as the side-to-thickness ratio, $t/b$, increases. Conversely, for plates with constant thickness, the frequency parameter decreases for plates with higher aspect ratio, $a/b$. Comparing the frequency parameters, $\lambda$, for plates with different boundary conditions, it is evident that plates with more constraints imposed on the boundaries have a higher value of $\lambda$. For example, the frequency parameters of the SFSF plate are generally many times higher than the corresponding modes of the CCCC plate with the same geometrical specifications.

Table 3(a). Comparison of frequency parameters, $\lambda = (\omega b^2/\pi^2)(\rho t/D)^{1/2}$, for a thick square plate with SSSS boundaries

| $t/b$ | Method of solution | Mode sequence number | | | | | |
|---|---|---|---|---|---|---|---|
| | | 1 (SS-1) | 2 (SA-1) | 3 (AS-1) | 4 (AA-1) | 5 (SS-2) | 6 (SS-3) |
| 0.01 | Classical theory† | 2.000 | 5.000 | 5.000 | 8.000 | 10.000 | 10.000 |
| | SDPT Ritz method‡ | 1.999 | 4.995 | 4.995 | 7.988 | 9.981 | 9.981 |
| | Present three-dimensional analysis | 1.9993 | 4.9956 | 4.9956 | 7.9888 | 9.9826 | 9.9826 |
| 0.1 | Classical theory† | 2.000 | 5.000 | 5.000 | 8.000 | 10.000 | 10.000 |
| | SDPT Ritz method‡ | 1.931 | 4.605 | 4.605 | 7.064 | 8.605 | 8.605 |
| | Three-dimensional exact analytical solution§ | 1.9342 | 4.6222 | 4.6222 | 7.1030 | 8.6618 | 8.6618 |
| | Present three-dimensional analysis | 1.9342 | 4.6222 | 4.6222 | 7.1030 | 8.6617 | 8.6617 |

†Leissa (1973).
‡Dawe *et al.* (1985) with a shear correction factor $\kappa = \pi^2/12$.
§Srinivas *et al.* (1970).

Table 3(b). Comparison of frequency parameters, $\hat{\lambda} = (\omega b'^2/\pi^2)(\rho t'/D)^{1/2}$, for a cantilevered thick square plate with $t'/b' = 0.5$

| Symmetry classes | Source of data | Mode sequence number | | | | |
|---|---|---|---|---|---|---|
| | | 1 | 2 | 3 | 4 | 5 |
| SS | Leissa and Zhang† | 1.0689 | 1.8733 | 2.1424 | 2.9200 | 3.1784 |
| | Present three-dimensional analysis‡ | 1.0687 | 1.8722 | 2.1394 | 2.8193 | 3.1260 |
| SA | Leissa and Zhang | 0.2996 | 1.1144 | 1.5253 | 2.2726 | 2.5327 |
| | Present three-dimensional analysis | 0.2976 | 1.1087 | 1.5222 | 2.2536 | 2.3608 |
| AS | Leissa and Zhang | 0.4469 | 1.1882 | 2.0545 | 2.8513 | 3.1962 |
| | Present three-dimensional analysis | 0.4449 | 1.1863 | 2.0369 | 2.7005 | 3.1616 |
| AA | Leissa and Zhang | 0.5279 | 1.4863 | 2.3028 | 2.5429 | 2.9916 |
| | Present three-dimensional analysis | 0.5263 | 1.4795 | 2.2772 | 2.4919 | 2.8482 |

†The values presented in this case are converted from the frequency results for a parallelepiped of configuration *C* in the paper by Leissa and Zhang (1983).

‡For this case, the following transformation has been done: $a' = t$, $b' = b$ and $t' = a$. This is to enable the comparison between the present three-dimensional analysis results and that of the reference for each symmetry class.

Table 4(a). Frequency parameters, $\lambda = (\omega b^2/\pi^2)(\rho t/D)^{1/2}$, for a thick plate with SSSS boundary condition

| Aspect ratio, $a/b$ | Thickness ratio, $t/b$ | Symmetry classes and mode number | | | | | | | | | | | |
|---|---|---|---|---|---|---|---|---|---|---|---|---|---|
| | | SS-1 | SS-2 | SS-3 | SA-1 | SA-2 | SA-3 | AS-1 | AS-2 | AS-3 | AA-1 | AA-2 | AA-3 |
| 0.5 | 0.01 | 4.9956 | 12.971 | 28.854 | 16.950 | 24.892 | 40.710 | 7.9888 | 19.930 | 39.724 | 19.930 | 31.823 | 51.535 |
| | 0.1 | 4.6222 | 10.879 | 14.587 | 6.5234 | 13.644 | 18.658 | 7.1030 | 13.047 | 15.597 | 13.047 | 15.596 | 22.610 |
| | 0.2 | 3.8991 | 7.2934 | 8.0926 | 3.2617 | 9.7636 | 9.7851 | 5.6524 | 6.5234 | 9.2255 | 6.5234 | 10.901 | 13.047 |
| | 0.3 | 3.2406 | 4.8623 | 6.2099 | 2.1745 | 6.5234 | 7.3431 | 4.3489 | 4.5123 | 6.1503 | 4.3489 | 8.1058 | 8.4528 |
| | 0.4 | 2.7254 | 3.6467 | 4.9705 | 1.6309 | 4.3912 | 4.8926 | 3.2617 | 3.6972 | 4.6127 | 3.2617 | 5.2213 | 6.3771 |
| | 0.5 | 2.3312 | 2.9174 | 3.8874 | 1.3047 | 2.9174 | 3.9140 | 2.6094 | 3.1080 | 3.6902 | 2.6094 | 3.6902 | 5.2187 |
| 1.0 | 0.01 | 1.9993 | 9.9826 | 9.9826 | 4.9956 | 12.971 | 16.950 | 4.9956 | 12.971 | 16.950 | 7.9888 | 19.930 | 19.930 |
| | 0.1 | 1.9342 | 8.6617 | 8.6617 | 4.6222 | 6.5234 | 10.879 | 4.6222 | 6.5324 | 10.879 | 7.1030 | 13.047 | 13.047 |
| | 0.2 | 1.7758 | 4.6127 | 6.6868 | 3.2617 | 3.8991 | 7.2934 | 3.2617 | 3.8991 | 7.2934 | 5.6524 | 6.5234 | 6.5234 |
| | 0.3 | 1.5895 | 3.0752 | 5.1152 | 2.1745 | 3.2406 | 4.8623 | 2.1745 | 3.2406 | 4.8623 | 4.3489 | 4.3489 | 4.5123 |
| | 0.4 | 1.4131 | 2.3064 | 3.7727 | 1.6309 | 2.7254 | 3.6467 | 1.6309 | 2.7254 | 3.6467 | 3.2617 | 3.2617 | 3.6972 |
| | 0.5 | 1.2590 | 1.8451 | 2.9325 | 1.3047 | 2.3312 | 2.9174 | 1.3047 | 2.3312 | 2.9174 | 2.6094 | 2.6094 | 3.1080 |
| 1.5 | 0.01 | 1.4441 | 4.9956 | 9.4289 | 2.7764 | 8.0996 | 10.758 | 4.4410 | 7.9888 | 15.071 | 5.7719 | 11.090 | 17.723 |
| | 0.1 | 1.4096 | 4.6222 | 7.8402 | 2.6538 | 6.5234 | 7.1916 | 4.1415 | 4.3489 | 7.1030 | 5.2834 | 8.6979 | 9.4988 |
| | 0.2 | 1.3209 | 3.8991 | 3.9201 | 2.3747 | 3.2617 | 5.4362 | 2.1745 | 3.5398 | 5.6524 | 4.3489 | 4.3818 | 6.5234 |
| | 0.3 | 1.2088 | 2.6134 | 3.2406 | 2.0731 | 2.1745 | 3.6241 | 1.4496 | 2.9719 | 4.3489 | 2.8993 | 3.5967 | 4.3489 |
| | 0.4 | 1.0954 | 1.9600 | 2.7254 | 1.6309 | 1.8064 | 2.7181 | 1.0872 | 2.5168 | 3.2617 | 2.1745 | 2.9998 | 3.2617 |
| | 0.5 | 0.9912 | 1.5680 | 2.3312 | 1.3047 | 1.5848 | 2.1745 | 0.8698 | 2.1631 | 2.6094 | 1.7396 | 2.5514 | 2.6094 |
| 2.0 | 0.01 | 1.2497 | 3.2482 | 7.2408 | 1.9993 | 4.9956 | 9.9826 | 4.2468 | 6.2432 | 10.232 | 4.9956 | 7.9888 | 12.971 |
| | 0.1 | 1.2237 | 3.0825 | 6.5003 | 1.9342 | 4.6222 | 6.5234 | 3.2617 | 3.9715 | 5.6785 | 4.6222 | 6.5234 | 7.1031 |
| | 0.2 | 1.1555 | 2.7197 | 3.6467 | 1.7758 | 3.2617 | 3.8991 | 1.6309 | 3.4110 | 4.6644 | 3.2617 | 3.8991 | 5.6524 |
| | 0.3 | 1.0669 | 2.3443 | 2.4311 | 1.5895 | 2.1745 | 3.0752 | 1.0872 | 2.8747 | 3.2617 | 2.1745 | 3.2406 | 4.3489 |
| | 0.4 | 0.9748 | 1.8233 | 2.0231 | 1.4131 | 1.6309 | 2.3064 | 0.8154 | 2.4409 | 2.4463 | 1.6309 | 2.7254 | 3.2617 |
| | 0.5 | 0.8881 | 1.4587 | 1.7624 | 1.2590 | 1.3047 | 1.8451 | 0.6523 | 1.9570 | 2.1018 | 1.3047 | 2.3312 | 2.6094 |

Table 4(b). Frequency parameters, $\lambda = (\omega b^2/\pi^2)(\rho t/D)^{1/2}$, for a thick plate with SFSF boundary condition

| Aspect ratio, $a/b$ | Thickness ratio, $t/b$ | Symmetry classes and mode number | | | | | | | | | | | |
|---|---|---|---|---|---|---|---|---|---|---|---|---|---|
| | | SS-1 | SS-2 | SS-3 | SA-1 | SA-2 | SA-3 | AS-1 | AS-2 | AS-3 | AA-1 | AA-2 | AA-3 |
| 0.5 | 0.01 | 3.9422 | 7.1459 | 17.096 | 15.834 | 19.355 | 29.991 | 4.7268 | 11.203 | 24.924 | 16.636 | 23.801 | 37.958 |
| | 0.1 | 3.6919 | 6.3161 | 13.099 | 12.849 | 13.047 | 15.098 | 4.3454 | 9.4257 | 11.401 | 6.5234 | 13.346 | 17.804 |
| | 0.2 | 3.1888 | 5.0595 | 6.5457 | 6.5234 | 9.2728 | 10.564 | 3.6651 | 5.6981 | 7.1055 | 3.2617 | 9.5497 | 9.7851 |
| | 0.3 | 2.7010 | 4.0572 | 4.3598 | 4.3489 | 7.0017 | 7.2482 | 3.0500 | 3.7967 | 5.4430 | 2.1745 | 6.5234 | 7.1780 |
| | 0.4 | 2.3019 | 3.2654 | 3.3227 | 3.2617 | 4.0771 | 5.2213 | 2.5665 | 2.8457 | 4.2216 | 1.6309 | 4.3912 | 4.8926 |
| | 0.5 | 1.9872 | 2.6071 | 2.7760 | 2.6094 | 2.6094 | 3.6902 | 2.1938 | 2.2750 | 3.2537 | 1.3047 | 2.9174 | 3.9140 |
| 1.0 | 0.01 | 0.9755 | 3.7118 | 8.8985 | 3.9422 | 7.1459 | 15.834 | 1.6316 | 7.6074 | 9.7065 | 4.7268 | 11.203 | 16.636 |
| | 0.1 | 0.9571 | 3.4361 | 7.7990 | 3.6919 | 6.3161 | 12.849 | 1.5603 | 4.9400 | 6.7287 | 4.3454 | 6.5234 | 9.4257 |
| | 0.2 | 0.9120 | 2.9650 | 4.6127 | 3.1888 | 5.0595 | 6.5234 | 1.4309 | 2.4697 | 5.3611 | 3.2617 | 3.6651 | 5.6981 |
| | 0.3 | 0.8523 | 2.5168 | 3.0752 | 2.7010 | 4.0572 | 4.3489 | 1.2855 | 1.6462 | 4.0872 | 2.1745 | 3.0500 | 3.7967 |
| | 0.4 | 0.7883 | 2.1469 | 2.3064 | 2.3019 | 3.2617 | 3.2654 | 1.1466 | 1.2344 | 3.0607 | 1.6309 | 2.5665 | 2.8457 |
| | 0.5 | 0.7261 | 1.8451 | 1.8502 | 1.9872 | 2.6071 | 2.6094 | 0.9874 | 1.0223 | 2.4421 | 1.3047 | 2.1938 | 2.2750 |
| 1.5 | 0.01 | 0.4303 | 2.9572 | 3.9422 | 1.7427 | 4.6687 | 7.0259 | 0.9714 | 4.7268 | 6.8664 | 2.4653 | 7.8310 | 8.5919 |
| | 0.1 | 0.4263 | 2.7835 | 3.6919 | 1.6882 | 4.2569 | 6.3055 | 0.9347 | 2.8075 | 4.3454 | 2.3345 | 6.5234 | 6.9192 |
| | 0.2 | 0.4165 | 2.4639 | 3.1888 | 1.5605 | 3.5823 | 5.0932 | 0.8744 | 1.4037 | 3.6651 | 2.0877 | 3.2617 | 3.5539 |
| | 0.3 | 0.4024 | 2.1386 | 2.2717 | 1.4082 | 2.9784 | 3.4727 | 0.8041 | 0.9357 | 3.0500 | 1.8272 | 2.1745 | 2.3686 |
| | 0.4 | 0.3854 | 1.7026 | 1.8575 | 1.2611 | 2.5007 | 2.6029 | 0.7018 | 0.7322 | 2.4346 | 1.5955 | 1.6309 | 1.7759 |
| | 0.5 | 0.3671 | 1.3608 | 1.6253 | 1.1303 | 2.0804 | 2.1280 | 0.5614 | 0.6634 | 1.9453 | 1.3047 | 1.4001 | 1.4203 |
| 2.0 | 0.01 | 0.2409 | 2.2096 | 2.6683 | 0.9755 | 3.7118 | 3.9422 | 0.6955 | 2.9542 | 6.5973 | 1.6316 | 4.7268 | 7.6074 |
| | 0.1 | 0.2396 | 2.1245 | 2.5338 | 0.9571 | 3.4361 | 3.6919 | 0.6704 | 1.8041 | 2.7800 | 1.5603 | 4.3454 | 4.9400 |
| | 0.2 | 0.2363 | 1.9318 | 2.2705 | 0.9120 | 2.9650 | 3.1889 | 0.6319 | 0.9021 | 2.4516 | 1.4309 | 2.4697 | 3.2617 |
| | 0.3 | 0.2315 | 1.7138 | 1.7309 | 0.8523 | 2.5168 | 2.7011 | 0.5866 | 0.6014 | 2.1178 | 1.2855 | 1.6462 | 2.1745 |
| | 0.4 | 0.2255 | 1.2975 | 1.5130 | 0.7883 | 2.1469 | 2.3019 | 0.4510 | 0.5389 | 1.8307 | 1.1466 | 1.2344 | 1.6309 |
| | 0.5 | 0.2185 | 1.0372 | 1.3409 | 0.7261 | 1.8451 | 1.8502 | 0.3608 | 0.4918 | 1.5947 | 0.9874 | 1.0223 | 1.3047 |

Table 4(c). Frequency parameters, $\lambda = (\omega b^2/\pi^2)(\rho t/D)^{1/2}$, for a thick plate with CFCF boundary condition

| Aspect ratio, $a/b$ | Thickness ratio, $t/b$ | Symmetry classes and mode number | | | | | | | | | | | |
|---|---|---|---|---|---|---|---|---|---|---|---|---|---|
| | | SS-1 | SS-2 | SS-3 | SA-1 | SA-2 | SA-3 | AS-1 | AS-2 | AS-3 | AA-1 | AA-2 | AA-3 |
| 0.5 | 0.01 | 9.0106 | 11.107 | 19.556 | 24.7583 | 27.462 | 36.467 | 9.4530 | 14.348 | 26.871 | 25.338 | 31.116 | 43.640 |
| | 0.1 | 7.2293 | 8.5641 | 14.376 | 16.4894 | 17.975 | 21.521 | 7.4881 | 10.813 | 12.465 | 16.795 | 19.984 | 21.721 |
| | 0.2 | 5.0464 | 5.8943 | 7.9491 | 10.1690 | 10.792 | 11.204 | 5.1893 | 6.2356 | 7.4674 | 10.394 | 10.886 | 11.934 |
| | 0.3 | 3.7236 | 4.3710 | 5.2917 | 7.1633 | 7.2055 | 7.5883 | 3.8180 | 4.1586 | 5.5462 | 7.2653 | 7.3540 | 7.9545 |
| | 0.4 | 2.9186 | 3.4558 | 3.9580 | 5.4107 | 5.4909 | 5.6878 | 2.9862 | 3.1198 | 4.3002 | 5.4537 | 5.6536 | 5.9660 |
| | 0.5 | 2.3917 | 2.8549 | 3.1536 | 4.3351 | 4.4336 | 4.5483 | 2.4417 | 2.4962 | 3.3877 | 4.3686 | 4.5690 | 4.7731 |
| 1.0 | 0.01 | 2.2482 | 4.4083 | 12.153 | 6.1972 | 8.8531 | 18.171 | 2.6743 | 8.0653 | 12.813 | 6.7985 | 12.560 | 20.754 |
| | 0.1 | 2.1050 | 3.9234 | 9.7276 | 5.3859 | 7.3581 | 10.636 | 2.4489 | 5.9500 | 6.9678 | 5.8272 | 10.070 | 10.961 |
| | 0.2 | 1.7996 | 3.1909 | 5.8790 | 4.1062 | 5.3313 | 5.4625 | 2.0363 | 2.9770 | 5.4325 | 4.4084 | 5.4824 | 6.5929 |
| | 0.3 | 1.4999 | 2.6089 | 3.9111 | 3.1647 | 3.5611 | 4.2065 | 1.6639 | 1.9858 | 4.2608 | 3.4031 | 3.6551 | 4.3999 |
| | 0.4 | 1.2582 | 2.1845 | 2.9226 | 2.5321 | 2.6747 | 3.3843 | 1.3764 | 1.4901 | 3.3581 | 2.7373 | 2.7411 | 3.3028 |
| | 0.5 | 1.0723 | 1.8710 | 2.3245 | 2.0957 | 2.1419 | 2.7196 | 1.1601 | 1.1926 | 2.6078 | 2.1928 | 2.2801 | 2.6439 |
| 1.5 | 0.01 | 0.9962 | 3.1862 | 5.3948 | 2.7473 | 5.3058 | 8.9231 | 1.3854 | 6.0511 | 7.0044 | 3.3250 | 9.0535 | 9.6178 |
| | 0.1 | 0.9662 | 2.9499 | 4.8158 | 2.5666 | 4.6977 | 7.0765 | 1.3078 | 3.7620 | 5.3192 | 3.0464 | 7.1685 | 7.7199 |
| | 0.2 | 0.8900 | 2.5456 | 3.8222 | 2.1871 | 3.5451 | 3.7823 | 1.1576 | 1.8825 | 4.1692 | 2.5419 | 3.5842 | 4.9930 |
| | 0.3 | 0.7971 | 2.1730 | 3.0331 | 1.8189 | 2.3673 | 3.0590 | 0.9989 | 1.2559 | 3.2938 | 2.0914 | 2.3893 | 3.3311 |
| | 0.4 | 0.7064 | 1.8718 | 2.4780 | 1.5234 | 1.7778 | 2.5333 | 0.8585 | 0.9425 | 2.6862 | 1.7455 | 1.7918 | 2.4998 |
| | 0.5 | 0.6262 | 1.6336 | 2.0845 | 1.2967 | 1.4238 | 2.1448 | 0.7419 | 0.7544 | 2.2531 | 1.4333 | 1.4854 | 2.0007 |
| 2.0 | 0.01 | 0.5589 | 2.7687 | 3.0281 | 1.5411 | 4.0182 | 5.0121 | 0.9099 | 3.6643 | 6.6554 | 2.0845 | 5.6985 | 7.8148 |
| | 0.1 | 0.5492 | 2.6076 | 2.8300 | 1.4811 | 3.6575 | 4.5324 | 0.8677 | 2.6560 | 3.3596 | 1.9573 | 5.0707 | 5.2162 |
| | 0.2 | 0.5224 | 2.3071 | 2.4174 | 1.3367 | 2.6556 | 3.0720 | 0.7884 | 1.3291 | 2.8090 | 1.7135 | 2.6083 | 4.0462 |
| | 0.3 | 0.4863 | 2.0014 | 2.0265 | 1.1718 | 1.7728 | 2.5614 | 0.6994 | 0.8868 | 2.3183 | 1.4672 | 1.7389 | 2.8676 |
| | 0.4 | 0.4470 | 1.6983 | 1.7567 | 1.0205 | 1.3311 | 2.1648 | 0.6147 | 0.6656 | 1.9409 | 1.2581 | 1.3042 | 2.1514 |
| | 0.5 | 0.4086 | 1.4556 | 1.5471 | 0.8925 | 1.0660 | 1.8593 | 0.5238 | 0.5400 | 1.6559 | 1.0434 | 1.0890 | 1.7215 |

Table 4(d). Frequency parameters, $\lambda = (\omega b^2/\pi^2)(\rho t/D)^{1/2}$, for a thick plate with SCSC boundary condition

| Aspect ratio, $a/b$ | Thickness ratio, $t/b$ | Symmetry classes and mode number | | | | | | | | | | | |
|---|---|---|---|---|---|---|---|---|---|---|---|---|---|
| | | SS-1 | SS-2 | SS-3 | SA-1 | SA-2 | SA-3 | AS-1 | AS-2 | AS-3 | AA-1 | AA-2 | AA-3 |
| 0.5 | 0.01 | 5.5434 | 15.650 | 33.653 | 17.208 | 26.748 | 44.641 | 9.5727 | 23.681 | 40.350 | 20.868 | 34.698 | 56.511 |
| | 0.1 | 5.0011 | 12.181 | 19.749 | 6.5234 | 13.749 | 19.242 | 8.0513 | 15.490 | 17.020 | 13.047 | 15.940 | 23.357 |
| | 0.2 | 4.0824 | 8.4898 | 9.8690 | 3.2617 | 9.7851 | 9.7942 | 6.0268 | 7.7475 | 11.230 | 6.5234 | 10.993 | 13.047 |
| | 0.3 | 3.3294 | 6.3451 | 6.5625 | 2.1745 | 6.5234 | 7.3552 | 4.6670 | 5.1663 | 7.9246 | 4.3489 | 8.1406 | 8.4528 |
| | 0.4 | 2.7722 | 4.8824 | 5.0262 | 1.6309 | 4.3912 | 4.8926 | 3.7700 | 3.8753 | 5.6207 | 3.2617 | 5.2213 | 6.3963 |
| | 0.5 | 2.3586 | 3.7834 | 4.1444 | 1.3047 | 2.9174 | 3.9140 | 3.1006 | 3.1478 | 4.0526 | 2.6094 | 3.6902 | 5.2187 |
| 1.0 | 0.01 | 2.9351 | 10.339 | 13.064 | 5.5434 | 15.650 | 17.208 | 7.0228 | 14.174 | 21.052 | 9.5727 | 20.868 | 23.681 |
| | 0.1 | 2.7188 | 8.8528 | 10.386 | 5.0011 | 6.5234 | 12.181 | 6.0522 | 11.451 | 11.517 | 8.0513 | 13.047 | 15.490 |
| | 0.2 | 2.2920 | 6.1314 | 6.7564 | 3.2617 | 4.0824 | 8.4898 | 4.5949 | 5.7649 | 8.2744 | 6.0268 | 6.5234 | 7.7475 |
| | 0.3 | 1.9061 | 4.0798 | 5.2688 | 2.1745 | 3.3294 | 6.3451 | 3.5633 | 3.8466 | 5.7845 | 4.3489 | 4.6670 | 5.1663 |
| | 0.4 | 1.6085 | 3.0494 | 4.2600 | 1.6309 | 2.7722 | 4.3912 | 2.8783 | 2.8868 | 4.3110 | 3.2617 | 3.7700 | 3.8753 |
| | 0.5 | 1.3836 | 2.4259 | 3.5114 | 1.3047 | 2.3586 | 2.9174 | 2.3106 | 2.4048 | 3.4078 | 2.6094 | 3.1006 | 3.1478 |
| 1.5 | 0.01 | 2.5399 | 5.5434 | 12.403 | 3.5574 | 8.5053 | 13.720 | 6.5866 | 9.5727 | 16.174 | 7.6568 | 12.406 | 20.868 |
| | 0.1 | 2.3661 | 5.0011 | 9.5615 | 3.2742 | 6.5234 | 7.4293 | 5.7058 | 8.0513 | 10.964 | 6.5548 | 10.178 | 12.531 |
| | 0.2 | 2.0040 | 4.0824 | 4.7802 | 2.7447 | 3.2617 | 5.8069 | 4.3400 | 5.4909 | 6.0268 | 4.9626 | 6.2705 | 6.5234 |
| | 0.3 | 1.6635 | 3.1849 | 3.3294 | 2.1745 | 2.2813 | 4.5959 | 3.3557 | 3.6651 | 4.6670 | 3.8557 | 4.1827 | 4.3489 |
| | 0.4 | 1.3966 | 2.3860 | 2.7722 | 1.6309 | 1.9269 | 3.7311 | 2.7003 | 2.7512 | 3.7700 | 3.1216 | 3.1383 | 3.2617 |
| | 0.5 | 1.1945 | 1.9054 | 2.3586 | 1.3047 | 1.6583 | 2.9174 | 2.2023 | 2.2488 | 3.0509 | 2.5114 | 2.6094 | 2.6123 |
| 2.0 | 0.01 | 2.4157 | 3.9605 | 7.6757 | 2.9351 | 5.5434 | 10.339 | 6.4378 | 8.0526 | 11.610 | 7.0228 | 9.5727 | 14.174 |
| | 0.1 | 2.2562 | 3.6311 | 6.7664 | 2.7188 | 5.0011 | 6.5234 | 5.5877 | 6.8672 | 9.5920 | 6.0522 | 9.0513 | 11.504 |
| | 0.2 | 1.9163 | 3.0302 | 4.1889 | 2.2920 | 3.2617 | 4.0824 | 4.2531 | 5.1889 | 5.4515 | 4.5949 | 5.7649 | 6.0268 |
| | 0.3 | 1.5907 | 2.5120 | 2.7920 | 1.9061 | 2.1745 | 3.3294 | 3.2841 | 3.6395 | 4.0321 | 3.5633 | 3.8466 | 4.3489 |
| | 0.4 | 1.3329 | 2.0930 | 2.1175 | 1.6085 | 1.6309 | 2.7723 | 2.6375 | 2.7322 | 3.2654 | 2.8783 | 2.8868 | 3.2617 |
| | 0.5 | 1.1369 | 1.6731 | 1.8190 | 1.3047 | 1.3836 | 2.3586 | 2.1871 | 2.1926 | 2.6394 | 2.3106 | 2.4048 | 2.6094 |

Table 4(e). Frequency parameters, $\lambda = (\omega b^2/\pi^2)(\rho t/D)^{1/2}$, for a thick plate with CCCC boundary condition

| Aspect ratio, $a/b$ | Thickness ratio, $t/b$ | Symmetry classes and mode number | | | | | | | | | | | |
|---|---|---|---|---|---|---|---|---|---|---|---|---|---|
| | | SS-1 | SS-2 | SS-3 | SA-1 | SA-2 | SA-3 | AS-1 | AS-2 | AS-3 | AA-1 | AA-2 | AA-3 |
| 0.5 | 0.01 | 9.9497 | 18.092 | 35.148 | 25.803 | 33.523 | 49.639 | 12.874 | 25.554 | 46.765 | 28.643 | 40.518 | 60.831 |
| | 0.1 | 7.9005 | 13.338 | 22.805 | 17.106 | 21.343 | 22.527 | 9.9367 | 16.844 | 17.740 | 18.705 | 23.636 | 24.887 |
| | 0.2 | 5.5132 | 8.9311 | 12.380 | 10.591 | 11.292 | 13.235 | 6.8531 | 8.4309 | 11.464 | 11.634 | 11.836 | 14.302 |
| | 0.3 | 4.0896 | 6.5367 | 8.1891 | 7.4983 | 7.5327 | 8.9245 | 5.0651 | 5.6229 | 8.2569 | 7.8979 | 8.2774 | 9.5149 |
| | 0.4 | 3.2202 | 5.1244 | 6.0222 | 5.6509 | 5.7686 | 6.6869 | 3.9796 | 4.2169 | 5.8684 | 5.9294 | 6.3782 | 7.1029 |
| | 0.5 | 2.6471 | 4.2077 | 4.6085 | 4.5247 | 4.6676 | 5.3330 | 3.2664 | 3.3723 | 4.2887 | 4.7504 | 5.1361 | 5.5589 |
| 1.0 | 0.01 | 3.6492 | 13.315 | 13.379 | 7.4352 | 16.682 | 21.266 | 7.4352 | 16.682 | 21.266 | 10.953 | 24.441 | 24.543 |
| | 0.1 | 3.3215 | 10.498 | 10.598 | 6.3457 | 12.522 | 12.706 | 6.3457 | 12.522 | 12.706 | 8.9030 | 14.870 | 17.275 |
| | 0.2 | 2.7261 | 7.3241 | 7.4249 | 4.7725 | 6.2735 | 8.6980 | 4.7725 | 6.2735 | 8.6980 | 6.4185 | 7.4370 | 9.1342 |
| | 0.3 | 2.2158 | 5.4605 | 5.5398 | 3.6707 | 4.1879 | 6.4322 | 3.6707 | 4.1879 | 6.4322 | 4.8493 | 4.9591 | 6.0860 |
| | 0.4 | 1.8330 | 4.3267 | 4.3868 | 2.9412 | 3.1431 | 5.0322 | 2.9412 | 3.1431 | 5.0322 | 3.7200 | 3.8580 | 4.5544 |
| | 0.5 | 1.5496 | 3.5774 | 3.6235 | 2.4396 | 2.5151 | 3.6545 | 2.4396 | 2.5151 | 3.6545 | 2.9765 | 3.1926 | 3.6285 |
| 1.5 | 0.01 | 2.7393 | 6.7420 | 12.682 | 4.2284 | 10.209 | 14.027 | 6.7002 | 10.441 | 18.042 | 8.0835 | 13.768 | 21.963 |
| | 0.1 | 2.5431 | 5.8780 | 10.109 | 3.8264 | 8.5057 | 9.6435 | 5.7899 | 8.6010 | 11.568 | 6.8531 | 10.936 | 12.655 |
| | 0.2 | 2.1476 | 4.5495 | 7.0982 | 3.1151 | 4.8272 | 6.2571 | 4.3954 | 5.7975 | 6.2870 | 5.1334 | 6.3321 | 7.7459 |
| | 0.3 | 1.7814 | 3.5676 | 5.1284 | 2.5198 | 3.2215 | 4.7786 | 3.3924 | 3.8710 | 4.7901 | 3.9525 | 4.2236 | 5.1637 |
| | 0.4 | 1.4939 | 2.8965 | 3.8322 | 2.0794 | 2.4177 | 3.8223 | 2.7232 | 2.9059 | 3.8298 | 3.1689 | 3.1755 | 3.8692 |
| | 0.5 | 1.2748 | 2.4262 | 3.0435 | 1.7558 | 1.9348 | 3.1283 | 2.2617 | 2.3257 | 3.0977 | 2.5359 | 2.6417 | 3.0894 |
| 2.0 | 0.01 | 2.4933 | 4.5396 | 8.8403 | 3.2278 | 6.4186 | 11.781 | 6.4836 | 8.4348 | 12.519 | 7.2010 | 10.205 | 15.364 |
| | 0.1 | 2.3261 | 4.1014 | 7.5448 | 2.9728 | 5.6514 | 8.4158 | 5.6221 | 7.1317 | 10.124 | 6.1823 | 8.4577 | 11.803 |
| | 0.2 | 1.9751 | 3.3346 | 5.7012 | 2.4842 | 4.2111 | 4.4350 | 4.2764 | 5.3356 | 5.6317 | 4.6763 | 5.9089 | 6.2218 |
| | 0.3 | 1.6420 | 2.6998 | 4.1330 | 2.0487 | 2.8091 | 3.5106 | 3.3001 | 3.7605 | 4.1125 | 3.6140 | 3.9429 | 4.7599 |
| | 0.4 | 1.3783 | 2.2328 | 3.0951 | 1.7133 | 2.1077 | 2.8659 | 2.6478 | 2.8231 | 3.3088 | 2.9085 | 2.9591 | 3.5754 |
| | 0.5 | 1.1770 | 1.8906 | 2.4688 | 1.4600 | 1.6866 | 2.4068 | 2.1985 | 2.2594 | 2.6779 | 2.3684 | 2.4217 | 2.8581 |

A set of vibration mode shapes for thick square plates with thickness ratio, $t/b = 0.2$, are presented in Figs 2–6. These correspond respectively to SSSS, SFSF, CFCF, SCSC and CCCC boundary conditions. The normalized transverse deflection ($W$-mode shape) and in-plane deflections ($U$- and $V$-mode shapes) are presented in shaded contour plots. The shaded portions in these figures represent regions with negative deflection amplitude while the unshaded portions represent regions with positive deflection amplitude. The lines of demarcation form the nodal lines for that particular mode.

By dividing the plates into regular meshes and assigning the vectorial displacement components $U$, $V$ and $W$ to each mesh coordinate, sets of three-dimensional deformed mode shapes are obtained. These diagrams express vividly the vibratory motion of the elastic plate at each mode of vibration. For all the boundary constraints examined in this study, it is observed that in general, the first doubly symmetric mode is predominantly an out-of-plane flexural motion in the $z$-direction. In addition, the through thickness deformations can also be seen for plates with edges that are free or simply supported. These through thickness deformations take on the form of either thickness-twisting or thickness-shearing motions, depending on the shapes of the deformed geometries. Figures 2(a) and 2(b) depict the deformed modes of a simply supported plate. It is observed that the symmetric flexural motions occur at the first and third SS modes. The second SS mode is predominantly an in-plane stretching and contracting motion in the $x$- and $y$-directions. Other flexural modes can be identified in the second SA mode (also in the second AS mode because of symmetry) and the first AA mode, respectively.

It is interesting to examine the vibratory motion of plates with free edges. Figures 3 and 4 depict the vibratory motion of plates corresponding to SFSF and CFCF boundary conditions. Comparing the first three SS modes of vibration for both cases, it is observed that the deformations exhibit similar characteristics. For both boundary conditions, the fundamental SS mode is an out-of-plane deflection in the $z$-direction forming an arc shaped deformed geometry. The prominent in-plane motion is found in the third SS mode. A more complex coupling of both in-plane and out-of-plane deflections are manifested in the higher SA, AS and AA modes of vibration.

Vibration mode shapes for plates with lesser degrees of freedom are shown in Figs 5 and 6, respectively, with SCSC and CCCC boundary conditions. Modes with distinct thickness deformation in the $x$-direction ($u$-mode) can be observed for the plate with SCSC boundaries. For the fully clamped plate, however, the through thickness motions are completely restrained at the boundaries. The in-plane motions in the $x$-direction ($u$-mode of vibration) dominate at the second SS and AA modes as well as in the first SA mode of vibration for the plate with SCSC boundary condition. The vibratory motions for the fully clamped plate, however, are mainly out-of-plane motion in the $z$-direction with certain degrees of in-plane sketching within the plate domain.

## 4. CONCLUSIONS

A comprehensive study on the vibration analysis of thick rectangular plates based on the linear, three-dimensional elasticity theory has been presented. The analysis is performed using the polynomial-based Ritz energy approach. Sets of orthogonally generated polynomial functions were used to describe the spatial displacement components in $U$, $V$ and $W$. For this study, no simplifying assumption has been made on the displacement fields and on the strain distribution across the thickness, thus the method is capable of providing accurate frequency solutions to the natural vibration of moderately thick to very thick plates.

Convergence tests and comparison studies have been carried out to establish the rate of convergence and validate the degrees of accuracy of the present three-dimensional formulation. These studies demonstrate the computational efficiency and accuracy of the method in analysing the free vibration of thick rectangular plates. Extensive numerical results for homogeneous, thick plates with different combinations of boundary conditions, aspect ratios and thickness ratios have been presented. It is deduced that the frequency

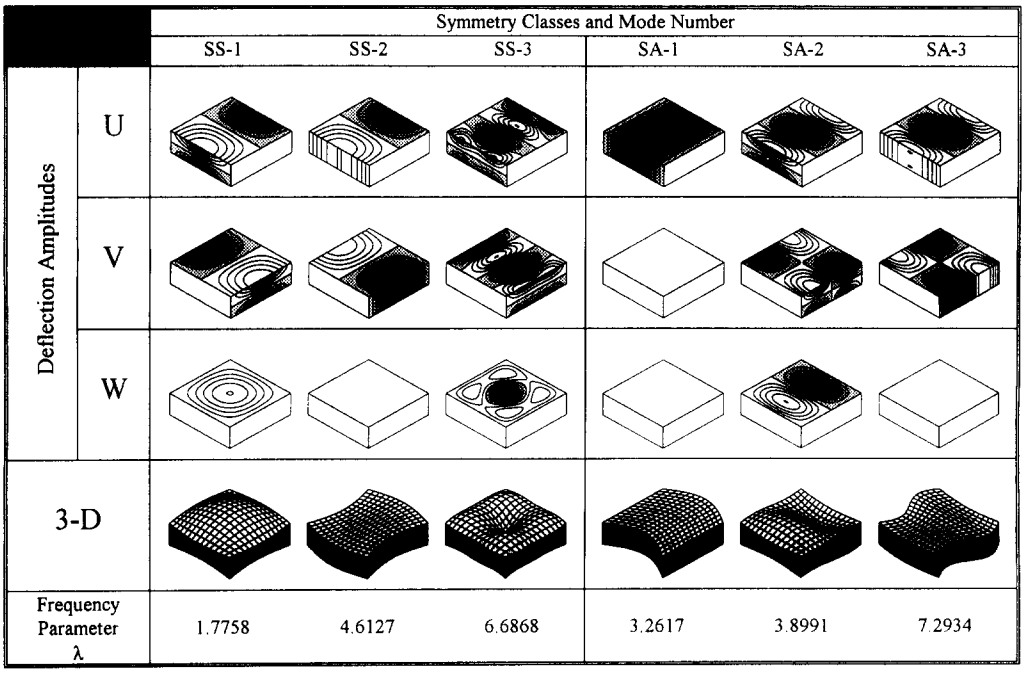


(a)

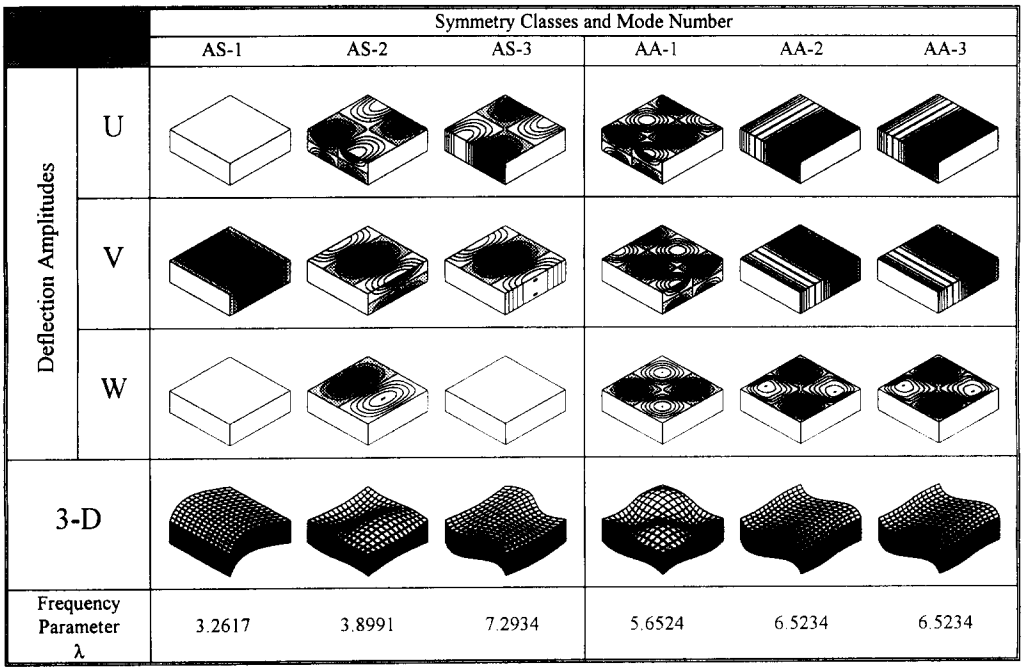


(b)

Fig. 2. Displacement contour plots and three-dimensional deformed geometry for the SSSS thick square plate with $t/b = 0.2$: (a) SS and SA modes; (b) AS and AA modes.

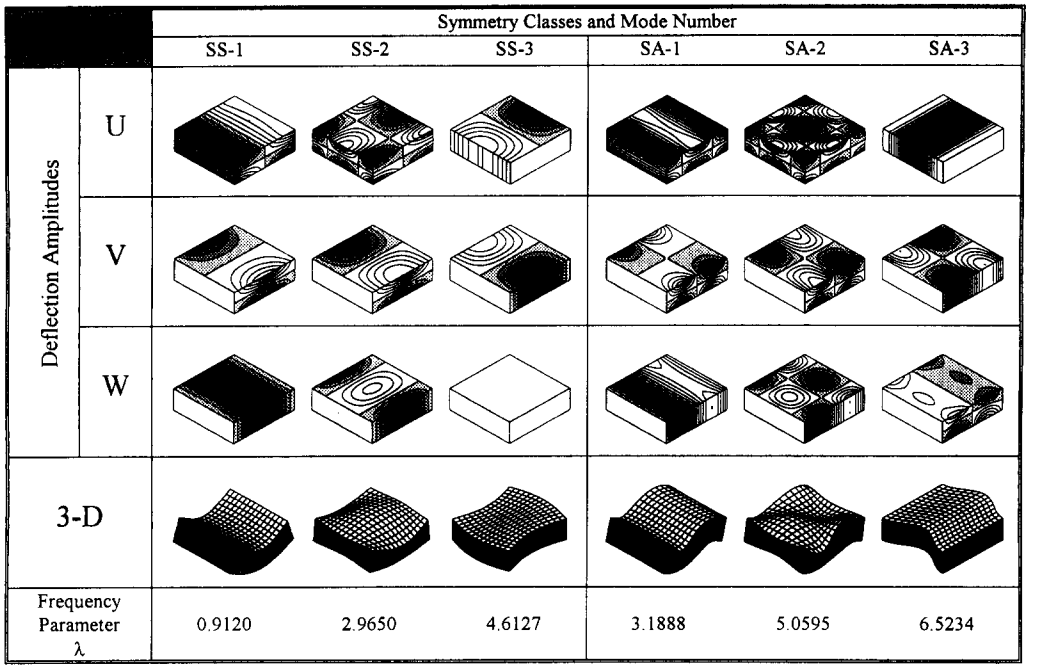


(a)

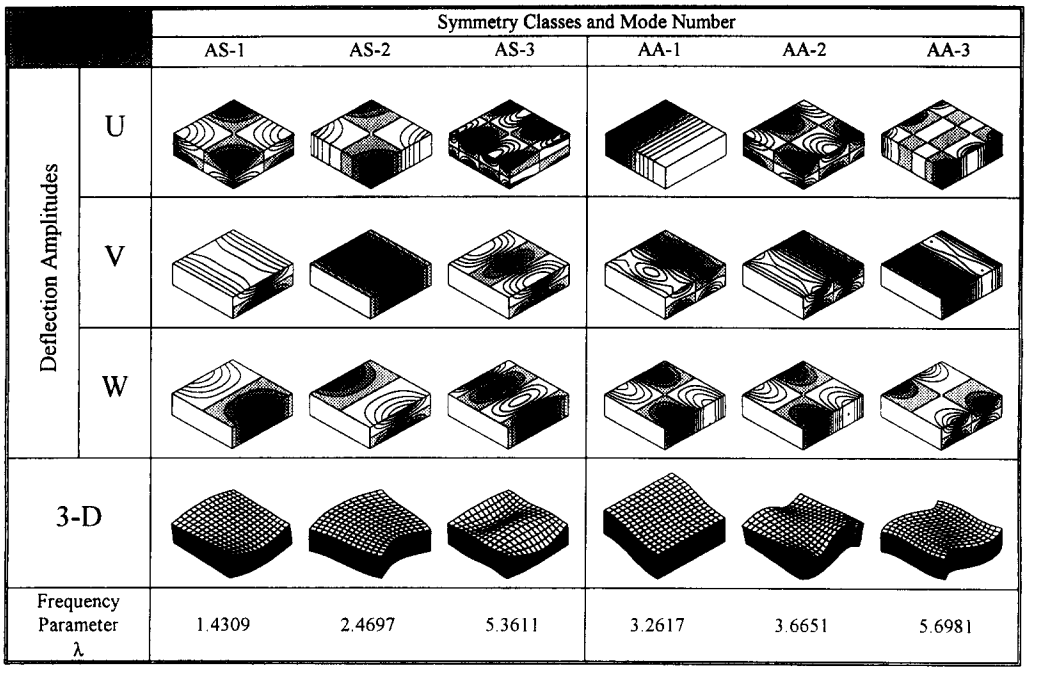


(b)

Fig. 3. Displacement contour plots and three-dimensional deformed geometry for the SFSF thick square plate with $t/b = 0.2$: (a) SS and SA modes; (b) AS and AA modes.

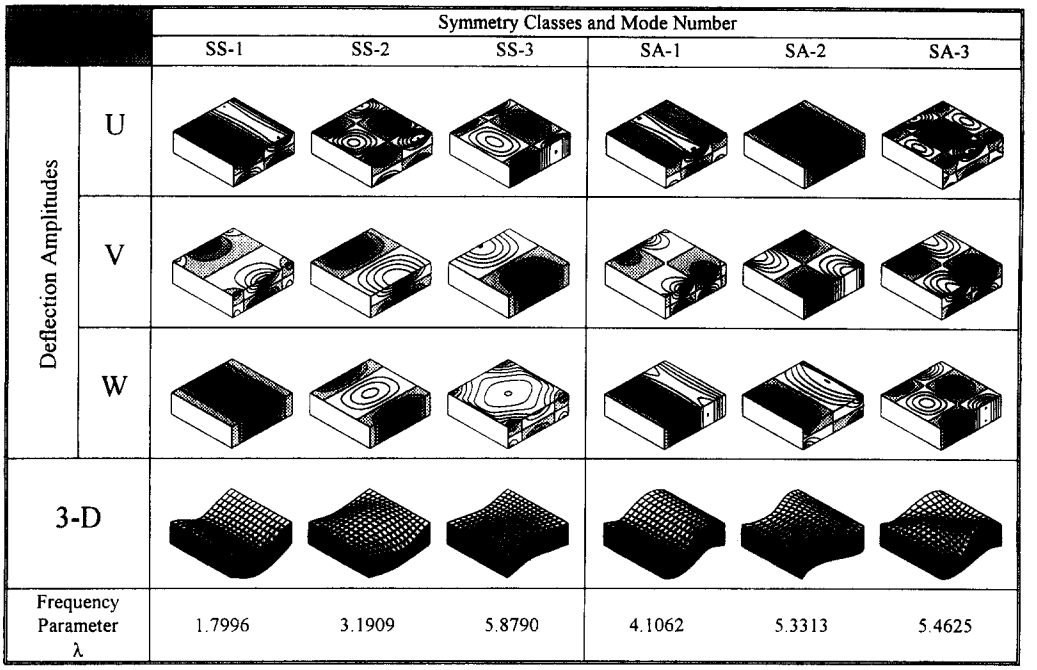


(a)

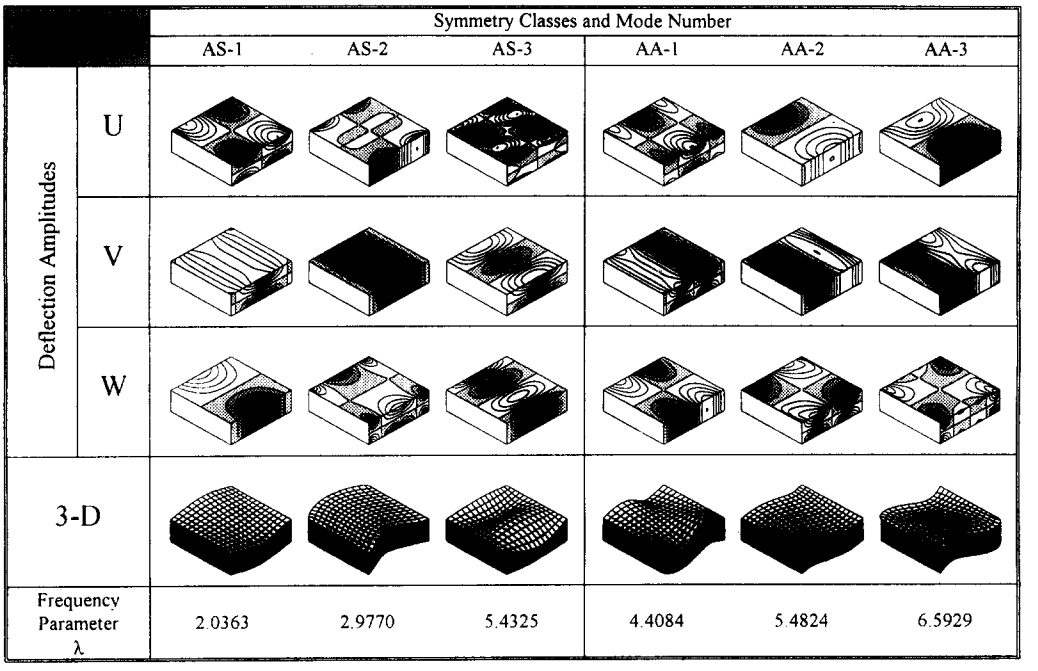


(b)

Fig. 4. Displacement contour plots and three-dimensional deformed geometry for the CFCF thick square plate with $t/b = 0.2$: (a) SS and SA modes; (b) AS and AA modes.

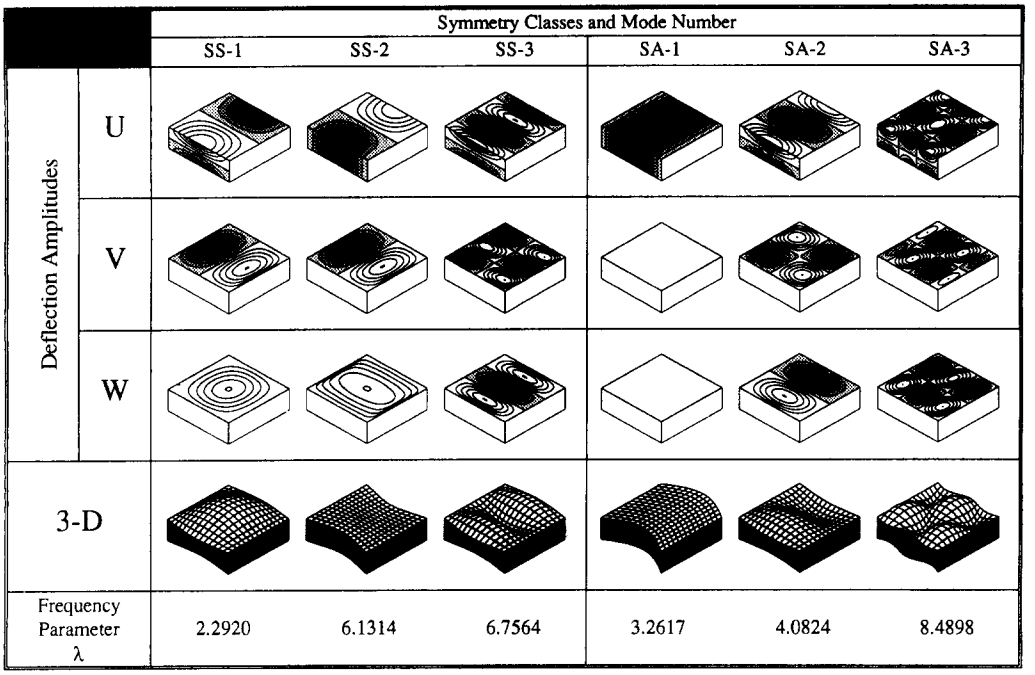


(a)

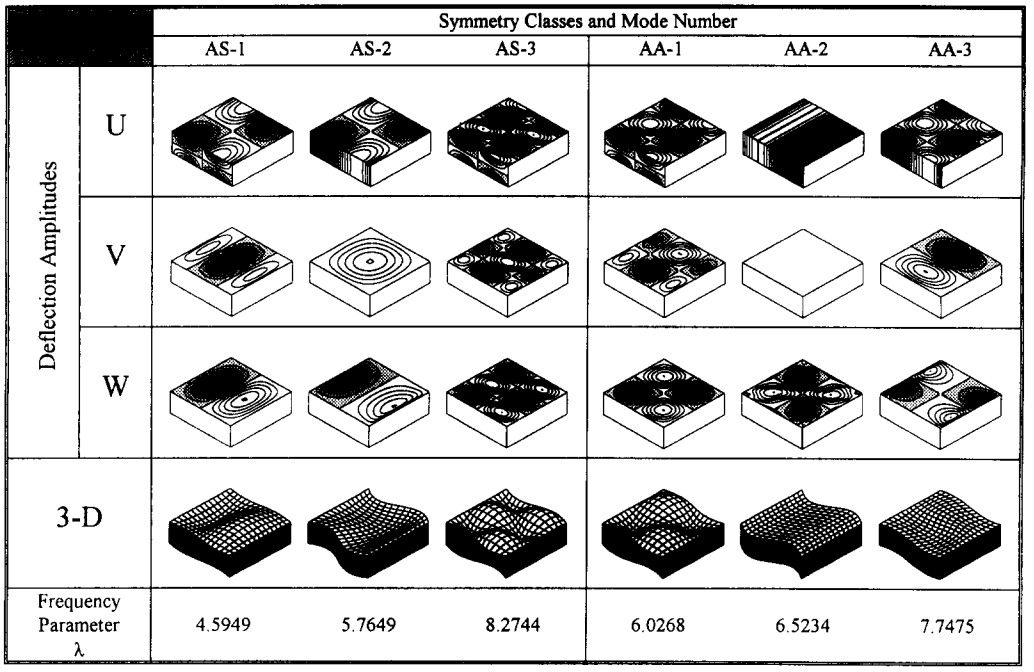


(b)

Fig. 5. Displacement contour plots and three-dimensional deformed geometry for the SCSC thick square plate with $t/b = 0.2$: (a) SS and SA modes; (b) AS and AA modes.

| | | Symmetry Classes and Mode Number | | | | | |
|---|---|---|---|---|---|---|---|
| | | SS-1 | SS-2 | SS-3 | SA-1 | SA-2 | SA-3 |
| Deflection Amplitudes | U | 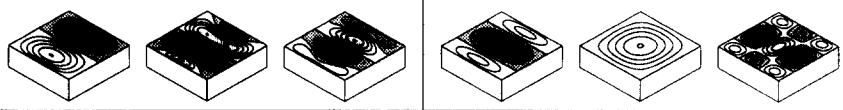 | | | | | |
| | V | 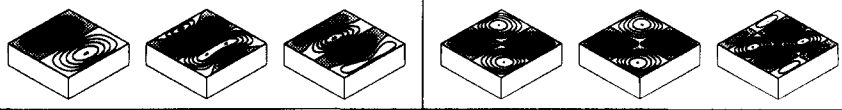 | | | | | |
| | W | 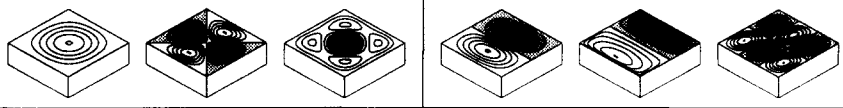 | | | | | |
| 3-D | | 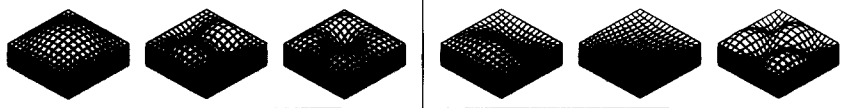 | | | | | |
| Frequency Parameter λ | | 2.7261 | 7.3241 | 7.4249 | 4.7725 | 6.2735 | 8.6980 |

(a)

| | | Symmetry Classes and Mode Number | | | | | |
|---|---|---|---|---|---|---|---|
| | | AS-1 | AS-2 | AS-3 | AA-1 | AA-2 | AA-3 |
| Deflection Amplitudes | U | 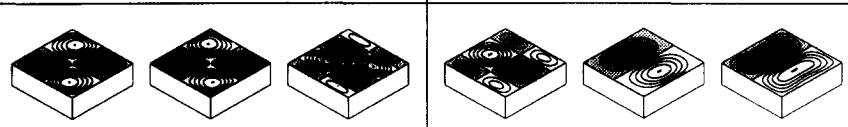 | | | | | |
| | V | 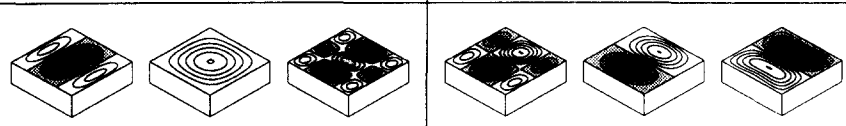 | | | | | |
| | W | 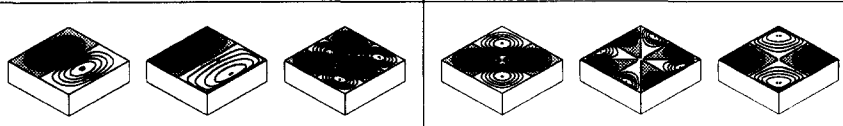 | | | | | |
| 3-D | | 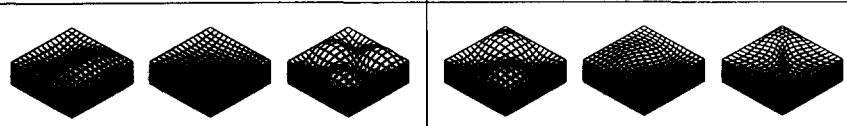 | | | | | |
| Frequency Parameter λ | | 4.7725 | 6.2735 | 8.6980 | 6.4185 | 7.4370 | 9.1342 |

(b)

Fig. 6. Displacement contour plots and three-dimensional deformed geometry for the CCCC thick square plate with $t/b = 0.2$: (a) SS and SA modes; (b) AS and AA modes.

parameters increase for plates with lower aspect ratio and smaller thickness ratio. The presence of more boundary constraints has increased the flexural stiffness, thus increasing the vibration frequencies.

Vivid representation of the vibration mode shapes are manifested in shaded contour plots and three-dimensional deformed mesh geometry. Through these deformed mode shapes, we have achieved a better understanding of the dynamic characteristics of these thick rectangular plates. These modes encompass the flexural, thickness twist and thickness shear motions which could also be identified in the approximate theories. In addition, the present three-dimensional elasticity formulation is capable of predicting those modes of vibration in which the approximation plate theories are found inadequate to predict. This concluding remark, in effect, agrees with the observation reported in the pioneering work of Srinivas *et al.* (1970).

## REFERENCES


Bhat, R. B. (1985). Natural frequencies of rectangular plates using characteristic orthogonal polynomials in the Rayleigh–Ritz method. *J. Sound Vibr.* **114,** 493–499.

Chihara, T. S. (1978). *An Introduction to Orthogonal Polynomials.* Gordon and Breach, New York.

Dawe, D. J., Horsington, R. W., Kamtekar, A. G. and Little, G. H. (1985). *Aspects of the Analysis of Plate Structures.* Clarendon Press, Oxford.

Dawe, D. J. and Roufaeil, O. L. (1980). Rayleigh–Ritz vibration analysis of Mindlin plates. *J. Sound Vibr.* **69,** 345–359.

Hutchinson, J. R. and Zillmer, S. D. (1983). Vibration of a Free Rectangular Parallelepiped. *ASME J. Appl. Mech.* **50,** 123–130.

Kao, R. (1973). Approximate solutions by utilizing hill functions. *Comput. Structs* **3,** 397–412.

Leissa, A. W. (1973). The free vibration of rectangular plates. *J. Sound Vibr.* **31,** 257–293.

Leissa, A. W. and Zhang, Z. D. (1983). On the three-dimensional vibrations of the cantilevered rectangular parallelepiped. *J. Acoust. Soc. Am.* **73,** 2013–2021.

Levinson, M. (1980). An accurate simple theory of the statics and dynamics of elastic plates. *Mech. Res. Commun.* **7,** 343–350.

Liew, K. M., Lam, K. Y. and Chow, S. T. (1990). Free vibration analysis of rectangular plates using orthogonal plate function. *Comput. Structs* **34,** 79–85.

Liew, K. M., Xiang, Y. and Kitiporchai, S. (1993). Transverse vibration of thick rectangular plates—I: comprehensive sets of boundary conditions. *Comput. Structs* (in press).

Narita, Y. (1985). The effect of point constraints on transverse vibration of cantilevered plates. *J. Sound Vibr.* **102,** 305–313.

Reddy, J. N. (1984). A simple higher-order theory for laminated composite plates. *ASME J. Appl. Mech.* **51,** 745–752.

Srinivas, S., Rao, C. V. Joga and Rao, A. K. (1970). An exact analysis for vibration of simple-supported homogeneous and laminated thick rectangular plates. *J. Sound Vibr.* **12,** 187–199.

Warburton, G. B. (1954). The vibration of rectangular plates. *Proc. Institution of Mechanical Engineers,* **168,** 371–384.

Wittrick, W. H. (1987). Analytical three-dimensional elasticity solutions to some plate problems, and some observations on Mindlin's plate theory. *Int. J. Solids Structs* **23,** 441–464.

Young, D. (1950). Vibration of rectangular plates by the Ritz method. *ASME J. Appl. Mech.* **17,** 448–453.